An edited version of this article appeared in:
R. D. Goldman and D. L. Spector, editors. Live Cell Imaging: A Laboratory Manual.
Cold Spring Harbor, NY: Cold Spring Harbor Laboratory Press. p 205-37. (2005)

November 2003

Polarization microscopy with the LC-PolScope

Rudolf Oldenbourg
Marine Biological Laboratory, Woods Hole, MA 02543, USA

Rudolf Oldenbourg
Marine Biological Laboratory
7 MBL Street
Woods Hole, MA 02543, USA
Tel: 508-289-7426
Fax: 508-540-6902
e-mail: rudolfo@mbl.edu

Table of Contents

Introduction

Most of the imaging approaches discussed in this Lab Manual are based on the use of fluorescent molecules and their detection inside living cells. Only a decade ago, live cell imaging was dominated by techniques such as phase contrast, differential interference contrast and polarized light microscopy which do not require the introduction of exogenous dyes or markers. Fluorescence microscopy, on the other hand, often required the killing and fixation of cells and then labeling them to detect specific molecular species. This role reversal was made possible by the many spectacular advances in fluorescence imaging and the development of many vital molecular probes, particularly the green fluorescent protein, which have seemingly outshined the more traditional techniques which probe the subtle changes of phase and amplitude of light that has interacted with the specimen. The phase sensitive techniques create images of living cells based on their intrinsic optical properties, in particular their refractive index. While the limelight was on fluorescence imaging, the more traditional techniques for live cell imaging have made great gains as well and they remain indispensable as complementary tools for imaging cell structure and function without the need for introducing fluorescent molecules into cells (Inoué and Spring, 1997; Sluder and Wolf, 1998).

Polarization microscopy uses polarized light to probe the local anisotropy of the specimen optical properties, such as birefringence or dichroism. These optical properties, which we will discuss in more detail later, have their origin in molecular order, i.e. in the alignment of molecular bonds or fine structural form in the specimen. Hence, polarization microscopy provides structural information at a submicroscopic level, including the alignment of molecules in filament arrays and membrane stacks such as the mitotic spindle, f-actin arrays, and retinal rod outer segments. Therefore, the polarizing microscope not only gives us information about where and when certain structures form and change inside the living cell, but also some of the submicroscopic features of these structures. Most importantly for live cell imaging, the polarizing microscope can do so dynamically both in short and long time periods, at the highest resolution of the light microscope, and with minimal interference with the physiological conditions required for the maintenance of live and healthy cells.

The use of the polarizing microscope for studying living cells was pioneered more than 70 years ago by W. J. Schmidt whose many original observations were published in a celebrated monograph (Schmidt, 1937). Intrigued by Schmidt's observations and Ambronn and Frey (Ambronn and Frey, 1926), and Frey-Wyssling studies (Frey-Wyssling, 1953), other groups began to use and refine the technique for live cell imaging, in particular for the phenomenon of cell division (Inoué, 1952; Inoué, 1953; Inoué and Dan, 1951; Inoué and Hyde, 1957; Mitchison, 1950; Swann and Mitchison, 1950), for a recent review of polarized light microscopy of spindles see (Oldenbourg, 1999)). For a discussion of the traditional polarized light microscope and its many uses in cell biology, the reader is referred to a recent article by Shinya Inoué, who for more than 50 years is the technique's strongest proponent ((Inoué, 2002), see also Appendix III in the first edition of (Inoué, 1986)).

In the current chapter we describe the use of a new type of polarized light microscope which we started to develop at the Marine Biological Laboratory about ten years ago. The new "PolScope" is based on the traditional polarized light microscope and enhances it with the use of liquid-crystal devices and special image processing algorithms. The LC-PolScope measures polarization optical parameters in many specimen points simultaneously, in fast time intervals, and at

the highest resolution of the light microscope. It rapidly generates a birefringence map whose pixel brightness is directly proportional to the local optical anisotropy, unaffected by the specimen orientation in the plane of view, as well as a map depicting the slow axis orientation of the birefringent regions. The basic LC-PolScope technology can be adapted to most research grade microscopes and is available commercially from Cambridge Research and Instrumentation (CRI, http://www.cri-inc.com) in Woburn, Massachusetts, under the trade name LC-PolScope.

The advantage of the LC-PolScope over the traditional polarizing microscope rests in its speed, sensitivity and accuracy. As Shinya Inoué likes to point out, for a seminal study on DNA organization in sperm heads it took him and two colleagues three years to analyze the polarized light images of three living cave cricket sperm (Inoué and Sato, 1966). A similar analysis would take seconds using the LC-PolScope. It must be said that the LC-PolScope measures specimen properties that, in principle, can be measured with the traditional polarizing microscope. However, the vastly improved speed and completeness of measurement (birefringence parameters for all resolved specimen points simultaneously) make the LC-PolScope the instrument of choice for many studies that benefit of the analytic power and submicroscopic information gleaned from polarized light images. Nevertheless, in some cases the traditional polarizing microscope might suffice to provide the needed information, be it the organization of filaments, membranes or chromophores in living cells (see the aforementioned article by (Inoué, 2002)). The decision to use the LC-PolScope is sometimes based on observations with the traditional instrument. In some cases one can find relevant information in the literature (see for example the extensive bibliography in Appendix III in the first edition of (Inoué, 1986)), other times one might do the exploratory observations using the traditional instrument oneself. This chapter was written for experimental scientists who want to get a better understanding of the capabilities of the new instrument and those who wish to optimize their use of it.

In describing the use of the LC-PolScope for live cell imaging, we first discuss the basic instrument, including the optical, electronic and software components and the influence of their performance parameters on the sensitivity, resolution, and speed of LC-PolScope measurements. As with the traditional polarizing microscope, the LC-PolScope technology can be implemented using many different design variations either for adapting it to a special measurement set-up, for improving the performance of the instrument or for measuring different optical parameters in the specimen. In describing the design we included some of these design variations which can be implemented with a few modifications to the basic PolScope instrument. We continue the discussion with the description of the image acquisition and measurement procedures used in the LC-PolScope, and of its performance characteristics and how to measure them. A good understanding of these issues puts the experimenter in a better position for optimizing the performance of the instrument for the specific study at hand. Towards the end we present a number of LC-PolScope images of living cells to give examples of the current range of systems studied with this new incarnation of an old and powerful technique.

Throughout this chapter we will use polarization optical terms such as retardance and optic axis which might not be familiar to the reader. Therefore, at the end we compiled a glossary of polarization optical terms, including a brief outline of the optical concepts of birefringence and retardance and of their measurement using imaging optics.

We believe the LC-PolScope technology is only at the beginning of a bright future. In our own laboratory at the MBL and in collaboration with CRI we continue to advance the LC-PolScope technology. We are working on extending its measurement capabilities beyond bire-

fringence, including dichroism and fluorescence polarization. Especially for improving live cell imaging we are working on increasing the speed of measurement to reduce the possibility of image artifacts due to specimen movements. We are also developing methods to measure polarization optical parameters in 3-dimensions. Hand in hand with these advances in instrumentation we are developing analytical tools for the interpretation of image content and for image restoration. All these developments are aimed to further unlock the secrets of cell structure and function as displayed in the architectural dynamics in living cells (for updates on our activities see http://www.mbl.edu/research/resident/lab_oldenbourg.html).

Instrumentation

The LC-PolScope instrumentation includes optical and electronic components and software for image processing and analysis. We first discuss general considerations regarding the optical set-up and strategies for selecting optical components for achieving best results. We also discuss considerations for combining PolScope optical elements with other imaging modalities, notably differential interference contrast (DIC) and fluorescence imaging. Finally, the specimen can be considered one of the optical components. Therefore, we give a few guidelines for preparing specimens and specimen chambers that are suitable, or incompatible, for observations with polarized light.

The LC-PolScope technology discussed in this chapter is covered by a US patent (Oldenbourg and Mei, 1996) which is licensed to Cambridge Research and Instrumentation (CRI) in Woburn, Massachusetts, USA (http://.cri-inc.com). CRI developed a commercial version for cell biology under the trade name LC-PolScope. The LC-PolScope includes optical components that are inserted into a microscope stand. Most stands from major microscope manufactures are suitable and can be optimized using the guidelines discussed in this chapter. We have prepared our instrumentation guidelines with the commercial version of the LC-PolScope in mind. We also discuss design variations that can be considered by the more experienced user of the LC-PolScope equipment, sometimes in collaboration with CRI, which is committed to supporting their customers in new and unconventional uses of the instrument. Furthermore, the LC-PolScope technology is constantly expanded and improved upon by CRI and by our own research at the Marine Biological Laboratory.

Basic optical set-up

The optical design of the LC-PolScope builds on the traditional polarized light microscope introducing two essential modifications: the specimen is illuminated with nearly circularly polarized light and the traditional compensator is replaced by an electro-optic, universal compensator. The PolScope also requires the use of monochromatic light. In **Figure 1,** the schematic of the optical train shows the universal compensator located between the monochromatic light source (e.g. arc lamp with interference filter) and the condenser lens. The analyzer for circularly polarized light is placed after the objective lens. The universal compensator is built from two variable retarder plates and a linear polarizer (see text box **The Universal Compensator**). The variable retarder plates are implemented as electro-optical devices made from two liquid crystal plates. Each liquid crystal plate has a uniform retardance that depends on the voltage applied to the device. The voltage for each plate is supplied by an electronic controller box connected to the retarders. The retarder controller box includes a microprocessor that stores liquid crystal related parameters for control of the variable retarder plates. The controller box is

The Universal Compensator

The universal compensator is built from two liquid crystal devices **LC-A** and **LC-B**, each of which functions as a uniform linear retarder plate. The retardance of a single plate can be adjusted between about 50 nm and 800 nm by applying a voltage between 10 Volt (800 nm) and 40 Volt (50 nm) to the liquid crystal device (for a more detailed description of liquid crystal variable retarders see (Khoo and Wu, 1993)). When changing the voltage, only the retardance changes, while the orientation of the slow (or fast) birefringence axis remains fixed.

As indicated in **Figure 1**, the slow axes of the linear retarders are mutually oriented at 45° to each other. In addition, the universal compensator includes a linear sheet polarizer (**polar**) whose transmission axis is oriented at 45° to the slow axis of **LC-A**. The polarizer and two liquid crystal plates are bonded together to form a thin optical flat with antireflection coatings on each side. The clear aperture can be 25 mm and larger and the stack is about 6 mm thick.

For measuring polarization optical properties of a specimen, the optical set-up also includes a circular polarizer. As indicated in Figure 1 and to the right here, a circular polarizer is typically built as a sequence of a linear sheet polarizer and a fixed quarter wave plate.

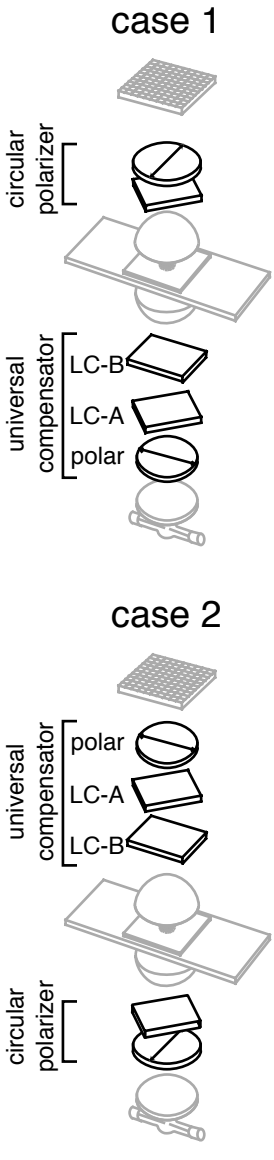

There are two basic choices for adding the universal compensator to the microscope optical train: Either before the condenser lens (**case 1** on the right, also shown in Figure 1), or after the objective lens (**case 2**). In both cases, the specimen (and high numerical aperture optics) is sandwiched between the universal compensator and the circular polarizer. Furthermore, the wave plates (the quarter wave plate of the circular polarizer and the LC wave plates of the universal compensator) are facing the specimen. Or, in other words, in both cases the linear polarizers are the first and last elements in the polarization optical train.

Hence, in either case, the specimen, high NA optics, and fixed and variable retarder plates are forming a polarization optical train sandwiched between two linear polarizers. This polarization optical train can be analyzed using mathematical descriptions known as Müller matrices and Stokes vectors. Based on such an analysis, we have developed image acquisition procedures and algorithms that allow one to use the PolScope for measuring polarization optical properties of the specimen in every resolved image point simultaneously (see **Retardance measurement**).

Both arrangements are equivalent in their ability to measure polarization optical parameters of the specimen. For the optical purist, though, **case 1** might be preferable to **case 2** which adds the universal compensator to the imaging path between objective and camera. Compared to the circular polarizer, the universal compensator represents a thicker optical flat and therefore might compromise the performance of the highly corrected objective lens. In practice, however, in most cases this difference is negligible.

Some additional optical properties, performance parameters and possible modifications to the universal compensator and circular polarizer are discussed under **Polarization optical components** and through out this chapter.

connected to a desk-top computer using a serial interface. The desk-top computer is also connected to the electronic camera, typically a CCD camera (charge coupled device), for recording the specimen images through the microscope optics. Specific software in the desk-top computer is designed to synchronize the image acquisition process with the liquid crystal control and to implement image processing algorithms that compute images representing the retardance and principal axis orientation in every resolved image point.

We want to emphasize, that during recordings of all four images in **Figure 1**, no part of the microscope set-up, including the specimen, was mechanically moved. To obtain the four images, only the voltages applied to the liquid crystal devices were changed. Therefore, all four images recorded with the CCD camera are in perfect register, with corresponding picture elements representing intensities of the same object elements. Optimal image registration is particularly important for measurements requiring high spatial resolution.

Design specifics and variances

Polarization optical components

Polarizers: The linear polarizers used in a PolScope should have high transmission and good extinction. Modern sheet polarizers are now available with transmission coefficients for unpolarized light of higher than 40% and extinction coefficients of around 10^4. An ideal polarizer has a transmission of 50% and infinite extinction. The extinction is a measure of the purity of the polarization state of light, after it has passed through the polarizer. The extinction coefficient is measured by the ratio of light transmitted through two polarizers in sequence, with their transmission axes aligned either parallel or perpendicular to each other (extinction = $I_{\parallel} / I_{\perp}$). Glan-Thompson and other prism polarizers perform close to the ideal values. For reasons given below good sheet polarizers are typically sufficient for the LC-PolScope.

The purity of the polarization in a light microscope is usually limited by the polarization distortions introduced by high numerical aperture condenser and objective lenses. While a pair of sheet polarizers might have an extinction ratio of 10^4 or higher, if a condenser and objective lens is placed between them, the extinction usually drops to around 10^3 or below (a pair of 1.4 NA oil immersion condenser and objective lenses has an extinction coefficient of around 200 if the condenser aperture diaphragm is fully open; partially closing the condenser aperture increases the extinction). Due to the development of calibration and correction procedures for the LC-PolScope, extinction plays a less critical role in the PolScope than in a traditional polarizing microscope. However, the sensitivity for measuring small retardance values that might be below 0.01 nm can be limited by the extinction of the set-up (see ***Performance characteristics and how to measure them***). In the following section, **Choice of optics**, we discuss the proper choice of lenses and refer to articles discussing the use of polarization rectifiers to minimize polarization distortions in high numerical aperture systems and optimize the performance of the LC-PolScope.

The circular polarizer used in the LC-PolScope is usually assembled from a linear polarizer and a quarter wave plate (see text box: **The Universal compensator**). Both components are made of thin polymer sheets of high optical quality that are bonded together. When inserting the circular polarizer in the optical path, care must be taken to insert it right side up. As illustrated in the text box **The Universal compensator**, the correct orientation depends on the arrangements illustrated in **case 1** and **case 2**. In either case, the quarter wave plate of the circular po-

larizer faces the specimen. For testing which side the quarter wave plate is on, one can use a separate linear polarizer. Looking through the circular and linear polarizer in tandem against a white light source, one rotates the two devices about their common normal axis and checks for extinction. Good extinction can only be achieved if the quarter wave plate is located outside the path between the two linear polarizers. If, however, the quarter wave plate is between the two linear polarizers, then different rotation angles result in differently colored light, but no extinction can be achieved.

While it matters to insert the circular polarizer right side up in the LC-PolScope optical train, it does not matter how it is rotated around the optical axis of the microscope. This is in stark contrast to a traditional polarizing microscope using linear polarizers which have to be carefully rotated to their crossed position. We leave it to the reader as an exercise to find an explanation for this peculiar feature of the LC-PolScope arrangement.

In a LC-PolScope with a straight optical path the circular polarizer usually transmits left circularly polarized light and absorbs right circularly polarized light. In some microscopes a mirror is present in the optical path between universal compensator and circular polarizer. Upon reflection by a mirror, circularly polarized light changes handedness. Therefore, in such a microscope the circular polarizer that is usually used in the LC-PolScope needs to be exchanged against one that transmits circularly polarized light of the opposite handedness. An even better solution is to rearrange the polarization elements in such a way that no mirror is in the optical path between them; because mirrors, like lenses, usually introduce polarization aberrations and reduce the extinction of the set-up.

Finally, we note that the circular polarizer is typically made for a specific wavelength, unless the quarter wave plate is specified for a range of wavelengths, a so-called achromatic quarter wave plate. If frequent changes between two or more wavelengths are necessary, one might consider using such an achromatic circular polarizer or obtain a tunable circular polarizer made, for example, of a linear polarizer and a liquid crystal variable retarder.

Universal compensator: The universal compensator is manufactured by Cambridge Research and Instrumentation and is made of two liquid crystal variable retarders and a linear polarizer (see text box: **The Universal compensator**). These components are usually bonded together and we assess their polarization optical performance as a unit. When considering the universal compensator as a unit by itself, it can also be called a *variable polarizer* based on the following property. When shining monochromatic light through the device so the light first passes through the linear polarizer followed by the two variable retarders, the light leaving the retarders can be made to have any desired polarization state, be it linear polarization of any azimuth or elliptical polarization of any handedness, ellipticity or azimuth (see equations 2,3,and 4 in (Shribak and Oldenbourg, 2003)). When shining light through the device in the opposite direction, so it first passes through the variable retarders and then through the linear polarizer, the device functions as a universal polarization analyzer. In this configuration extinction can be achieved for any input polarization by setting the retardance of the liquid crystal variable retarder plates to suitable values. Based on the retardance values needed for extinction, one can calculate the polarization of the incoming light using equations that are equivalent to the ones referred to earlier. This property can be used for some unconventional applications of the universal compensator. For example in fluorescence imaging, when inserting the universal compensator in the illumination path or imaging path (or both) the specimen can be illuminated with light of a specific polarization and/or the light from the specimen can be analyzed for any given polarization state.

With regard to the performance of the universal compensator, we give instructions on how to measure the extinction coefficient of the complete PolScope optical set-up in the section ***Performance characteristics and how to measure them***.

Apart from extinction and transmission, another important performance parameter of the universal compensator is the time required to reliably switch between two polarization states, the so-called settling time. The settling time is determined by the liquid crystal devices and is usually greater than 100 ms. However, faster settling times are possible and LC devices can be constructed with settling times of 30 ms and lower, usually at the expense of the range of retardance values that the devices can be adjusted to.

Choice of optics

As indicated earlier, the polarization distortions introduced by the objective and condenser lenses limit the extinction that can be achieved in a polarizing microscope. But not all lenses are created equal. Most microscope manufacturers offer lenses that are designated "Pol" to indicate low polarization distortions which can arise from a number of factors, including stress or crystalline inclusions in the lens glass and the type of antireflection coatings used on lens surfaces. Some lens types are not available with "Pol" designation, but with the designation "DIC". These lenses don't measure up to the more stringent Pol requirements but pass for the use of differential interference contrast and can also be used with the LC-PolScope (without the special Wollaston or Nomarski prisms, of course).

The polarization performance of the most highly corrected lenses, so called Plan Apochromat objectives, is often compromised due to the large number of lens elements, the special antireflection coatings, and in some cases the special types of glass used to construct the lenses (Inoué and Oldenbourg, 1995). For some applications of the LC-PolScope the Plan-Apochromat correction might be overkill anyway. If you plan to use the objective lens only with the PolScope that requires monochromatic light and typically acquires images from a region near the center of the viewing field, a correction lesser than Plan Apochromat might suffice. The special lens design for Plan Apochromats providing a large, highly corrected viewing field over a wide spectral range is often not required for LC-PolScope applications. To find out what works best for a particular imaging situation, we recommend to test a few lenses. For best performance, it is also helpful to be able to select the best performing pair of condenser and objective lens from a batch of the same lens types.

Whenever possible or practical, use oil immersion lenses. Oil, and to a lesser degree water and other immersion liquids, greatly reduce polarization aberrations caused by air-glass interfaces between the specimen and the lenses. The transition of a light ray between two media of different refractive index ($n_{air} = 1.00$, $n_{glass} = 1.52$) introduces polarization distortions, especially for high NA lenses. The peripheral rays leaving the condenser front lens are highly tilted to the slide surface and their polarization is typically rotated when traversing the air-glass interface (Inoué, 1952; Inoué and Hyde, 1957). For a discussion of the origin of polarization distortions in lenses and optical systems and of ways to reduce them we refer to a recent article by Shribak et al. (Shribak et al., 2002). The publication also discusses the various conoscopic images that can be observed in a polarizing microscope equipped with crossed, or nearly crossed polarizers and a Bertrand lens.

Lenses and other optical elements that are not placed between the universal compensator and the circular polarizer do not affect the extinction performance of the microscope set-up. Therefore, in a dissecting microscope for example, the polarizing elements and the liquid crystal devices might be better placed between the objective lens and the light source. The light source is typically an incandescent lamp with diffuser plate in the base of the dissecting scope. On top of the diffuser plate one can first place an interference filter followed by the fixed circular polarizer. The liquid crystals might be mounted in a special holder in front of the objective lens. In a dissecting microscope, the rays captured by the objective to project the image have small tilt angles (low NA). Hence, the rays passing through the liquid crystals have small enough tilt angles as not to compromise the polarization performance of the liquid crystals.

While optical elements placed outside the polarization optical train don't affect the extinction, they do contribute to the overall performance of the set-up. Aside from considerations regarding image quality, the sensitivity of measuring small retardance features in the specimen also depends on the proper match between the resolution of the optical image and of the electronic camera. We will address the relationship between resolution, sensitivity and speed of measurement in the section on ***Performance characteristics and how to measure them***.

Inverted microscope stand

Inverted stands equipped with the required optical components can be equally suited for polarized light microscopy as upright stands. Here are a few points to consider when using an inverted stand for the PolScope:

> Inverted stands frequently have a mirror in the optical path. A mirror has two effects: (1) the circular polarizer or analyzer might have to be exchanged for one with the opposite handedness, because circularly or elliptically polarized light changes handedness upon reflection by a mirror (only relevant if the mirror is in polarization optical path, between the universal compensator and the analyzer);
> (2) if the mirror is in the imaging path, the calculated azimuth angle needs to be inverted because of the change in symmetry of the raw LC-PolScope images. A checkbox named "Inverted microscope" is provided in the LC-PolScope software to include this final inversion step. If one failed to check the box and needs to correct the angle later, simply replace the old azimuth value φ by $(180 - \varphi)$.
>
> Plastic Petri-dishes, often used with inverted scopes, cannot be used with the PolScope. However, plastic Petri-dishes with a glass bottom are ok (see, for example, http://www.glass-bottom-dishes.com/).
>
> If your cell preparation is in a culture dish with a glass bottom, you might consider trans-illuminating your specimen using an immersion condenser that dips into the aqueous culture medium. A water immersable objective as condenser lens will give best results, but requires modifications to the condenser mounting. As an alternative, a regular oil immersion condenser can be dipped into the medium to avoid the air glass and air water interface and the concomitant polarization distortions of a dry condenser lens. It also provides for high NA illumination for improved resolution. Of course, in the process the sterility of the culture will be compromised. Also, one should carefully wipe the condenser dry after contacting it with an aqueous medium.

Culture chamber and heating stage

For a comprehensive discussion on culture chambers, heating stages and other accessories for keeping live cells happy while they are mounted on the microscope we refer to the **special chapters in this Lab Manual**. For observations using polarized light we want to point out the following issues:

> Absolutely avoid plastic components in the polarization optical path. Most plastic materials are highly birefringent and therefore greatly reduce the sensitivity and accuracy of the LC-PolScope measurement. In some cases it is possible to replace the plastic material with suitable glass components A case in point is the modified plastic Petri dish with glass bottom.
>
> Avoid equipment that introduces temperature gradients in objective and condenser lenses and in other optical components that are part of the polarization optical train of the microscope. Temperature gradients in glass cause stress and associated stress birefringence which reduces the sensitivity of the PolScope. Stress birefringence also introduces a background retardance that usually changes over time, modulating the calibration of the instrument.

Choice of light source

The PolScope requires a stable, bright, monochromatic light source. Depending on the application, the requirements can be met by a halogen lamp, an arc lamp (e.g. mercury or xenon), a light emitting diode (LED) or suitably scrambled laser light. For a more detailed discussion of light sources for live cell imaging we refer the reader to the chapter by **Phong Tran in this Lab Manual**. Here we briefly discuss the effect of different lamp characteristics on PolScope measurements.

Stability is paramount among the specifications for a light source suitable for the PolScope. The lamp intensity must be stable during the time period required for the exposure of a stack of raw PolScope images. For example, for measuring retardance values of around 0.1 nm using a standard LC-PolScope optimized for low retardance measurments, the lamp intensity must be stable within 1%. An unstable light source is tantamount to varying the exposure level between raw PolScope images which in turn has the same effect as introducing a uniformly birefringent plate in the polarization optical train. However, in some cases, PolScope images that were exposed using an unstable light source can be corrected after the fact using the background ratioing method discussed below under ***Background birefringence and how to correct it***.

Brightness is another important factor to consider in polarization microscopy. Obviously, the intensity of the light source is directly proportional to the time it takes to expose the camera detector to appropriate light levels. Furthermore, for measuring small retardance values, the PolScope is operated with settings of the universal compensator that are near extinction. Hence, the light level on the camera and in the eye piece for direct observations are low and it can become difficult to align the instrument and position and focus the sample correctly without sufficient light. Therefore, a bright light source is needed for an efficient work flow, especially when working with live cells. Since cells are sensitive to light the PolScope set-up should include a shutter that is conveniently operated and blocks the light to the specimen whenever possible. Blocking the light when it is not needed is an efficient way of reducing light damage to the cells.

The PolScope requires monochromatic light for its operation. Light with a spectral bandwidth of 30 nm is an upper limit and should not be exceeded without risking to loose sensitivity (increased spectral width reduces the extinction of the set-up). Therefore, most light sources, except for lasers, require an interference filter for selecting or narrowing the spectral range of the source. In contrast, a laser's spectral width is usually too narrow and its time coherence too long for wide field imaging (Inoué and Spring, 1997).

In our own experience, a 100W mercury arc lamp, as supplied by microscope manufacturers and equipped with a 546 nm interference filter (http://www.omegafilters.com or http://www.chroma.com), provides sufficiently bright, monochromatic light for measuring fast, dynamic events, such as spindle dynamics during mitosis. Other strong emission lines of a mercury arc lamp have center wavelengths of 577 nm and 436 nm and can also be used after exchanging the interference filter and circular polarizer suitable for the selected wavelength. Typically, when an arc burner is used longer than 150 hours, the gap between the electrodes increases and the shape of the tip of the electrodes often becomes irregular leading to an instable arc geometry. As a result, the brightness of the lamp starts to flicker. When lamp flickers become apparent by direct viewing, or the flickers can be recognized as elevated background retardance that changes erratically over time (see above), it is probably time to change the bulb. To improve resolution and minimize image artifacts we also use a fiber based Ellis light scrambler which is available from Technical Video, Ltd (http://www.technicalvideo.com/). Finally, there are several ways to adjust the amount of light delivered to the specimen, including a diaphragm that varies the light level entering the fiber optic light scrambler, and neutral density filters with calibrated attenuation factors. Avoid closing the condenser aperture to reduce the light level, because this will also decrease the resolution of the image.

In the future we expect light emitting diodes (LEDs) to replace traditional light sources for many applications, especially when monochromatic light is needed. Over the past several years, LEDs have improved significantly with respect to their brightness and now can provide higher intensity monochromatic light compared to halogen lamps. LEDs are highly efficient and stable light sources, whose brightness can be controlled by the source current. They can also be driven to provide short light pulses with peak powers that are several times the DC power limit (see for example http://.lumileds.com).

Combining the PolScope with DIC and fluorescence imaging

For differential interference contrast (DIC), two matching prisms are added to the polarization optical path (for a discussion of the standard DIC arrangement see (Salmon and Tran, 1998)). The two prisms, called Wollaston or Nomarski prisms, are specially designed to fit in specific positions, one before the condenser and the other after the objective lens, and to match specific lens combinations. The prisms in their regular positions can be combined with the PolScope set-up, in which case the universal compensator and circular analyzer take the places of the linear polarizer and analyzer in a standard DIC arrangement. In fact, the same DIC prisms function equally well using either linearly or circularly polarized light.

For best results, the PolScope is first calibrated without prisms to find the extinction setting for the universal compensator. With the compensator set to extinction, the prisms are entered into the optical path. Typically, one of the two prisms has a mechanism for fine-adjusting its position which in turn affects the brightness and contrast of the DIC image. In a PolScope set-up, one can either use the mechanical fine adjustment or one can use the universal compensator to add a bias

retardance to change the brightness and contrast of the DIC image. When using the universal compensator, one needs to add or subtract retardance from the extinction setting of either the **LC-A** or **LC-B** retarder (see **Figure 1**), depending on the orientation of the shear direction of the prisms.

For live cell imaging, we find it very useful to switch easily between PolScope and DIC imaging. DIC provides good contrast of many morphological features in cells using direct viewing through the eye piece or by video imaging. When viewing specimens that have low polarization contrast, we find it more effective to align the optics including the visualization of the specimen using DIC. After the optics are aligned and the specimen is in focus, the DIC prisms are removed from the optical path and the PolScope specific adjustments are completed.

Fluorescence imaging can be combined with the PolScope in several ways. Fluorescence is commonly observed using epi-illumination requiring a filter cube in the imaging path. The filter cube includes a dichromatic mirror and interference filters for separating the excitation and emission wavelengths. For best results the filter cube should be removed for PolScope observations to avoid the polarization distortions caused by the dichromatic mirror. For observing fluorescence, on the other hand, the PolScope analyzer should be removed, because it attenuates the fluorescence emission by at least 50%. To meet both requirements one can mount the PolScope analyzer in an otherwise empty filter cube holder which is moved into the optical path as the fluorescence cube is moved out, and vice versa.

If, however, the option of removing the fluorescence cube is unavailable, the cube can remain in the optical path for PolScope observations. In this case, consider the following points:

> For the light source of the PolScope choose a wavelength that is compatible with the emission wavelength filter in the fluorescence cube. For example, fluorescein isothiocyanate (FITC) requires excitation with blue light (485 nm) and fluoresces in the green. The FITC dichromatic beam splitter and barrier filter passing green fluorescence light with wavelength longer than 510 nm would be compatible with 546 nm light for PolScope observations using a mercury arc burner for the transmission light path.
>
> Calibrate the PolScope with the fluorescence filter cube in place. The polarization distortions caused by the dichromatic mirror are partially counteracted by the calibrated settings of the universal compensator.
>
> Make sure the light source for one imaging mode is blocked while observing with the other imaging mode.
>
> Removing the PolScope analyzer while observing fluorescence more than doubles the fluorescence intensity.

While beyond the scope of this article, it should be noted that the universal compensator can also be used to analyze fluorescence polarization. As described in the section on **Polarization optical components**, the universal compensator can also be regarded as a universal polarization analyzer or a universal polarizer. It can thus play a valuable role in selectively exciting or detecting polarized fluorescence. Fluorescence polarization imaging has become a powerful tool for probing structure together with functional aspects in living cells and working model systems. Fluorescence polarization can be used as binding assay of small and medium-sized molecules to receptors and other binding sites. (Peterman et al., 2001) and as probe to differentiate between

conformational states (Warshaw et al., 1998). The combination of molecular specificity and dynamic measurement of molecular orientation by fluorescence polarization analysis has revealed the rotational motion of actin filaments during sliding over myosin molecules fixed on a glass surface (Sase et al., 1997). Recently, Inoué and colleagues have discovered and analyzed the remarkable fluorescence polarization properties of single crystals of the green fluorescent protein (Inoué et al., 2002). As indicated in this paper, the highly polarized nature of GFP fluorescence provides a new method for dynamically observing, and quantifying, the changing orientation of fluorescent chromophores constituting (or attached to) functional molecular structures.

Specimen preparation

Last, but certainly not least, we consider the specimen and its mount as part of the polarization optical train. There are **several chapters in this Lab Manual** which discuss the preparation of viable cells suitable for observations in the light microscope. We also refer to the recent article by Shinya Inoué on polarized light microscopy in a Lab Manual for Cell Biology (Inoué, 2002). Also, our article on polarized light microscopy of spindles has a section on cell types suitable for live cell imaging of spindles and their preparation (Oldenbourg, 1999). Here we will give a few general pointers for making live cell preparations for the PolScope.

> Prepare the specimen so that when mounted in the microscope you can identify at least one clear area without cells or birefringent material and move it into the viewing field when required. A clear area is needed for calibrating the PolScope and for recording a PolScope stack of background images. The background images provide a record of the combined effect of the polarization properties of all optical components, including the slide and coverslip, but not of the specimen itsself. Using the background images, the spurious background retardance is removed from PolScope images of the cells and structures that you wish to measure precisely and image clearly. Many cell cultures or cell free systems are suitably prepared without special attention to this requirement. For example, a free area can often be found around cells that are sparsely plated on coverslips. Cultures of free swimming cells might have to be diluted appropriately before mounting a small drop between slide and coverslip. Sometimes we find it helpful to add a tiny drop of oil or other non-toxic, immiscible liquid to the preparation. The clear drop can provide an area for calibrating the instrument and take background images in a preparation that is otherwise dense with birefringent structures. For further discussions on collecting background images see ***Background birefringence and how to correct it*** and **Performance characteristics and how to measure them**.
>
> If your cells are round and small, the edge birefringence of the cell surface might be strong and obscure other detail. For reducing the edge birefringence you can add, polyethyleneglycol, polyvinylpyrrolidone, or some other harmless polymer or protein substitute to increase the medium's refractive index. The percent concentration of substitute required might vary from a few percent to 16% and more, depending on the average refractive index of the cytoplasm of the cells you are studying. It is best to make up a few trial solutions of media with different polymer concentrations, suspend the cells in them and look at a slide and coverslip prep with DIC or polarized light. At the right polymer concentration, the cells will look as if their internal organelles and cytoskeleton are suspended in space because you can see no distinct cell boundary.

After determining the concentration you should test the compatibility by growing cells in medium with polymer. Cells should grow and develop normally in media with these types of additives. The molecular weight of the polymer should be around 40 kD or more to prevent its uptake into cells.

Earlier in this chapter, we recommended the use of immersion optics whenever possible (see **Choice of optics**). When using high NA oil immersion optics, prepare specimens in which the cells or the structures of interest are as close to the coverslip as possible. A layer of more than 10 μm of aqueous medium introduces enough spherical aberration to noticeably reduce the resolution of cell images. The use of water immersion optics alleviates this problem (Inoué and Spring, 1997).

Finally, as discussed earlier, don't use a plastic dish to observe your specimen, unless the dish has a glass bottom (see **Inverted microscope stand**).

Image acquisition and measurement

After the optical components are aligned and the specimen is mounted correctly, it's time to take a picture. The appearance of raw PolScope images depends on the settings of the universal compensator. To illustrate the workings of the universal compensator, four different PolScope images of the same specimen are shown near the top of **Figure 1**. The specimen is an aster formed in lysate prepared from eggs of the surf clam (Palazzo et al., 1992). Asters are convenient test objects since their radially arranged microtubules lead to a spherically symmetric birefringence pattern. The centrosome in the middle of the picture shows little birefringence. The birefringence increases rapidly near the surface of the centrosome due to the increasing density of aligned microtubules. With increasing distance from the centrosome, the birefringence decreases from a few nanometer retardance to fractions of nanometer. The slow axis is oriented parallel to the direction of the radially arranged microtubule bundles. The top left image of **Figure 1** shows the specimen when it is illuminated with circularly polarized light. Astral rays appear bright, regardless of their orientation, against the dark background. Background light is blocked by the analyzer that has opposite circular handedness to the illuminating polarization. The following three images to the right show the specimen illuminated with elliptically polarized light. The ellipticity is the same for each of the three settings but the orientation of the principal axes of the polarization ellipse is rotated by multiples of 45°. The following section on calibration briefly describes what the four universal compensator settings are and how they are calibrated.

Calibration

Calibrating the LC-PolScope refers to optimizing the liquid crystal settings that are used to measure specimen retardance. For the calibration the specimen is usually moved sideways to view a clear area that has no retardance. Hence, when making the sample preparation, one should anticipate the need for clear areas adjacent to cells or other objects of interest (see **Specimen preparation**). If no clear area is available, then the alternative is to remove the specimen from the optical path. The calibration usually proceeds automatically, supported by the software that is part of the LC-PolScope instrument. We will briefly describe the calibration procedure.

With the clear area in view, the software (or user) selects a small region of interest (ROI) typically near the center of the image and measures the average intensity in that region. Subsequently, the retardance of one of the liquid crystal devices in the universal compensator is

slightly changed, a new intensity reading is taken and compared to the previous reading. The sequence of changing retardance and reading the intensity in the ROI repeats until the following settings are optimized:

Setting 1 (extinction): starting with nominal retardance values (λ/4, λ/2), the retardance of both LC-A and LC-B are changed until the intensity reading is at a minimum. We will call the pair of optimized retardance values ($R_{1,LC\text{-}A}$, $R_{1,LC\text{-}B}$). The optimized values are usually within 0.04 λ of the nominal values.

Setting 2: starting with Setting 1, a so-called "swing" retardance is added to LC-A. The swing retardance, or simply swing, is user selected and depends on the expected sample retardance values. For imaging living cells, the swing retardance is typically set to 0.03 λ or 16 nm (λ = 546 nm). After the swing retardance is added to LC-A, the intensity is read. This intensity is used as reference I_{ref} for optimizing the remaining settings. Setting 2 requires no further adjustments. Hence, the retardance pair of setting 1 is ($R_{1,LC\text{-}A}$ + Swing, $R_{1,LC\text{-}B}$).

Setting 3: starting from Setting 1, the swing retardance is added to LC-B and the intensity is read. Subsequently, LC-B is varied up or down in small steps until the measured intensity is equal to I_{ref} (LC-A is kept constant at $R_{1,LC\text{-}A}$). The resultant retardance pair of Setting 3 is ($R_{1,LC\text{-}A}$, ~ $R_{1,LC\text{-}B}$ + Swing), where the sign " ~ " indicates that the optimized value might vary from the start value.

Setting 4: starting from Setting 1, the swing retardance is subtracted from LC-B and the retardance of LC-B is varied in small steps until the measured intensity is equal to I_{ref}. The resultant retardance pair of Setting 4 is ($R_{1,LC\text{-}A}$, ~ $R_{1,LC\text{-}B}$ - Swing)

Recently, Michael Shribak has developed a series of algorithms that use from two Settings to five Settings of the universal compensator (Shribak and Oldenbourg, 2003). Adding the following 5th setting improves the sensitivity and accuracy of retardance measurements:

Setting 5: starting from Setting 1, the swing retardance is subtracted from LC-A and the retardance of LC-A is varied in small steps until the measured intensity is equal to I_{ref}. The resultant retardance pair of Setting 5 is (~ $R_{1,LC\text{-}A}$ - Swing, $R_{1,LC\text{-}B}$).

An abbreviated measurement process that uses only Settings 2 and 3 increases the speed but reduces image quality for preliminary examinations of birefringent specimens.

As discussed earlier, the universal compensator can be considered a variable polarizer. Setting 1 produces a circularly polarized light beam, while Settings 2 and higher produce elliptically polarized beams that each have equal ellipticity but differing orientations of the principal axes.

Retardance measurement

The images recorded of a birefringent specimen using the aforementioned Settings 1 through 5 of the universal compensator are evaluated for measuring the retardance in every resolved specimen point. The image algorithms used in the evaluation are integral to the software of the LC-PolScope system and have been published elsewhere (Shribak and Oldenbourg, 2003). Here, we briefly summarize the algorithms to give some insight into the relationship between the intensity values *I* measured by the camera in a given image point, the Swing value used in calibrating the liquid crystals and the sought-after retardance and azimuth values of a specimen region. We

base the summary on the original algorithm using the first four settings of the universal compensator.

We first define intermediate results A and B, based on the image intensities I_1 to I_4 and the Swing value χ expressed as a phase angle (e.g. for a Swing of 0.03 λ, $\chi = 0.03 \cdot 360° = 10.8°$):

$$A \equiv \frac{I_2 - I_3}{I_2 + I_3 - 2I_1} \cdot \tan\frac{\chi}{2},$$

$$B \equiv \frac{I_2 + I_3 - 2I_4}{I_2 + I_3 - 2I_1} \cdot \tan\frac{\chi}{2}$$

Using these intermediate results, expressions for the retardance R and azimuth φ are as follows:

$$R = \arctan\left[\sqrt{A^2 + B^2}\right] \quad \text{if } I_2 + I_3 - 2I_1 \geq 0,$$

$$R = 180 \ - \arctan\left[\sqrt{A^2 + B^2}\right] \quad \text{if } I_2 + I_3 - 2I_1 < 0,$$

$$\varphi = \frac{1}{2}\arctan\left(\frac{A}{B}\right).$$

The above formulas for the retardance and slow axis direction of a birefringent region apply to transparent specimens that posses linear birefringence. In the visible wavelength range and for non-absorbing biological specimens, linear birefringence is typically the dominant optical anisotropy. However, absorbing specimens recognized by their colored appearance, might possess dichroism that can affect retardance measurements. It is best to choose a wavelength for which the absorption is a minimum. Also, beware that the PolScope ambiguously measures retardance values above half a wavelength. For example, let us assume the specimen retardance $R_{specimen}$ is in the range $\lambda/2 < R_{specimen} < \lambda$. The measured retardance is then $R = \lambda - R_{specimen}$, and the azimuth angle is turned by 90°. For $\lambda < R_{specimen} < 3\lambda/2$, $R = R_{specimen} - \lambda$ and the measured azimuth angle is correct. A retardance in the range $0 < R_{specimen} < \lambda/2$ is measured correctly in both the retardance and azimuth value.

As discussed in the next section, it is necessary to distinguish between so-called instrument or background birefringence and the specimen birefringence that one actually wants to measure.

Background birefringence and how to correct it

After calibrating the instrument it is good practice to record a so-called background stack. **Figure 2** shows images of a clear area of a thin, aqueous sample sandwiched between microscope slide and coverslip. The images were recorded after the calibration procedure was completed. The features seen in the images are not part of the specimen, but are contributed by other components of the optical set-up. The retardance and azimuth image (panel 5 and 6 in **Figure 2**) were computed using the algorithm of the LC-PolScope software. In the retardance image one recognizes a dark streak crossing the center of the image. The dark center is a result of the calibration procedure which seeks settings for the liquid crystal universal compensator that result in

near zero retardance in the center of the image. The exact shape of the dark region varies between different microscope set-ups and depends on the lenses and other optical components used. Outside the dark area, the image shows a smoothly varying retardance background that increases with distance from the central area. This smooth retardance background is due to the residual polarization distortions introduced by optical components including the microscope objective and condenser lens. In addition to the smoothly varying background retardance, there are several localized retardance features which are the result of contaminations (dirt), blemishes and imperfections, sometimes located on surfaces near the camera face plate. All of these instrument or background retardance features have slow axis orientations associated with them as shown in panel 6 of **Figure 2**.

If uncorrected, the background retardance can cause deterioration of the images of the specimen which might have structures with retardance values that are one to two orders of magnitude smaller than the average background retardance. Therefore, we developed a background correction procedure that removes the effect of instrument birefringence on the measured specimen retardance.

Figure 3 shows retardance images of an oral epithelial cell (cheek cell) prepared by putting a drop of saliva between a slide and cover glass. Resolving the fine ridges on the surface of the cheek cell is a useful test for the achieved resolution and contrast in phase based microscopy, such as phase contrast, differential interference contrast and polarized light microscopy. **Figure 3** shows two retardance images, one without background correction and one with correction. The difference is remarkable and illustrates the need and the success of the background correction procedure.

The theory of the background correction procedure is described in detail elsewhere (Shribak and Oldenbourg, 2003). In practice, the background correction requires a stack of raw PolScope images of a clear area in the specimen prep. The retardance image in **Figure 3**, for example, was corrected using a background stack that was recorded after the cheek cell was moved to the side using the x-y translation stage of the microscope. For the typical experimental set-up, we recommend the following steps:

1. Calibrate the microscope with the specimen in place while viewing an adjacent clear area that has no specimen retardance.
2. With the clear area in view, acquire a background stack that records the retardance due to instrument parts only.
3. Move specimen under investigation into view.
4. Focus the object and acquire a sample stack that records the retardance of the object and of the instrument parts together.
5. When computing the object retardance, make sure that background correction is enabled and references the correct background stack.

The following points help to determine whether the background correction worked:

In the retardance image of the object, the birefringent parts appear bright against a dark, flat background.

When looking at background areas with suitable contrast enhancement, a random noise level is observed. The expected average retardance value of the noise level is discussed in **Performance characteristics and how to measure them**.

In the azimuth image, the background areas exhibit a random variation of the azimuth angle between 0° and 180°. This large range of random angles is very striking in azimuth images and serves as an easily recognizable indicator for the quality of the background correction.

The background correction procedure can use a single background stack repeatedly and can correct, for example, a time series of sample images measuring the subtle changes in birefringence in a living cell.

Here are some further hints for making the best use of background correction:

It might be time to record a new background stack when you notice that specimen parts that should have no retardance show some uniform retardance background. The uniform retardance background might be caused by a drift in the liquid crystal settings due to changes in room temperature, for example. (see below for background ratioing)

Defocus the background image slightly before acquiring a background stack. The defocus can avoid image features in the background stack that are due to blemishes on the coverslip surface, for example. Such features in the background stack will also show up in the background corrected sample image.

Use frame averaging for acquiring the background stack, even though you might not use frame averaging for acquiring the sample stack. Averaging reduces the noise level in images. The noise level in the final, background corrected sample image is the root mean square of the noise level in the background stack and the sample stack together.

The expected noise level in acquired and computed images is discussed in more detail under the heading **Performance characteristics and how to measure them**.

Finally, we want to mention a procedure called **background ratioing** which is used to further correct sample images. Background ratioing can be helpful in cases where background corrected sample images show an unwanted, uniform background retardance. The situation might arise while recording a time series of PolScope images, for example. Let us assume that the time series was recorded while the liquid crystal settings slowly drifted away from their calibrated values, due to a slow temperature increase in the room, for example. The background corrected sample images will then show a uniform background retardance that slowly increases from time point to time point. To avoid this situation, one might record a new background stack at appropriate time intervals. If, however, the recording of the time series prevents one from moving the specimen, or the intruding background retardance was only noticed after the recording, then background ratioing can come to the rescue.

Background ratioing requires a background stack, a sample stack, and an area within the sample image that has zero retardance. The a-priori knowledge that the identified sample area has zero retardance can be used to correct the entire sample stack. The correction modifies the intensity values in the raw PolScope images of the sample stack before calculating the retardance and azimuth images. Each of the raw PolScope images is modified separately following these

steps: (1) calculate the average intensities in the identified area of the sample image and the background image; (2) form the ratio (background/sample) of the average intensities; (3) multiply all intensities in the sample image with this ratio. After this modification of the sample stack, the retardance and azimuth images are calculated using the usual background correction procedure. It can be shown that the procedure successfully corrects any small sample retardance that was measured with incorrectly calibrated liquid crystals. In addition, the procedure also corrects errors due to an unstable light source that causes the exposure of individual raw PolScope images to be unequal (also see **Choice of light source**). Liquid crystal drifts and lamp flickers have similar effects on the computed retardance and azimuth images. Both can be suppressed by the background ratioing procedure.

Performance characteristics and how to measure them

After carefully aligning and optimizing the optical set-up and suitably preparing the specimen for the PolScope, what performance can you expect of your instrument?

The performance characteristics of the PolScope can be divided into four categories: sensitivity, accuracy, speed and resolution. Obviously, the four categories are interrelated and for maximizing one category one will have to sacrifice in another. In the following discussion we will include those relationships and give guidelines for optimizing specifications that are typically required for live cell imaging.

Resolution

The spatial resolution of the PolScope image is mainly determined by the optical lenses employed and their proper use and alignment. The numerical aperture of the objective lens NA_{obj} and of the condenser lens NA_{cond} are equally important in determining the minimum distance $d_{\min}$ of two object points that can still be separated in the image:

$$d_{\min} = \frac{\lambda}{NA_{obj} + NA_{cond}},$$

where λ is the wavelength of light used (Inoué and Oldenbourg, 1995). To actually achieve this optical resolution in your PolScope images consider the following points:

Observe the specifications provided by the manufacturer of the lenses including the required coverslip thickness (usually Nr. $1^1/_2$ or 0.17 mm) for the objective.

Each additional optical component (filter, polarizer, compensator etc.) in the imaging path should introduce less than a quarter wave wavefront distortion.

A high numerical aperture oil immersion objective gradually looses its nominal resolution when focusing into an aqueous layer of more than 10 µm thickness. Use water immersion (or water immersable) lenses for focusing deeper into cells or tissues.

When using high numerical aperture lenses in the PolScope, the condenser aperture should be partially closed to improve the sensitivity by increasing the extinction of the polarization optical train (see **Choice of Optics**). Using 1.4 NA oil immersion optics, for example, we usually close the condenser aperture down to 1.0 NA, choosing a compromise between reducing resolution and improving extinction.

The resolution of the final PolScope image is also determined by the camera resolution. A zoom lens before the camera provides some flexibility in adjusting the field size projected onto the camera face plate. We usually set the zoom factor so that the optical resolution matches the camera resolution, i.e. the distance $d_{\min}$ is spanned by 3 camera pixels (according to the Nyquist theorem, $d_{\min}$ should be spanned by at least 2 pixels). Under normal circumstances there is no benefit in choosing a larger zoom factor. However, a smaller zoom factor increases the brightness of the image and one might be able to reduce the exposure time enough to catch fast events in the cell. Thus, a zoom lens can provide the flexibility required to compromise between spatial and temporal resolution.

The resolution and distance calibration of a PolScope image can be measured using a number of different test objects:

1. The distance calibration is affected by the magnification of the objective and intermediate zoom lenses in the optical path. If all magnification factors are known, then the nominal distance calibration can be estimated by dividing the camera pixel size by the various magnification factors. For a reliable way of calibrating the image distance, one should image a micrometer scale available from microscope manufacturers and distributors.
2. To test the resolution, a single, submicroscopic point or line object, such as a microtubule (Oldenbourg et al., 1998), small calcite crystal (Oldenbourg and Török, 2000), and even a submicroscopic, isotropic scatterer like a latex bead or small organelle in a cell can be used. Even though the scatterer is isotropic, there is a residual edge effect that makes the retardance image of the submicroscopic bead look like a small donut (Török, 2000). Single, submicroscopic objects tend to have very low retardance, usually below 1 nm. The distance $d_{\min}$ can be estimated from the half width at half maximum of the retardance image of the submicroscopic object. A single point scatterer is also useful to test for the presence of spherical aberrations in the imaging optics. When spherical aberration is present, the defocused image looks different when changing the focus from above to below the point scatterer (for example, focusing into a water layer with an oil immersion objective introduces spherical aberration). Spherical aberration is the main cause of an asymmetric point spread function.
3. The silica shell of diatoms is studded with pores and markings that have species specific, regular distances. **Figure 4** shows the retardance image of a *Frustulia rhomboides* diatom with rows of pores that are 0.29 μm apart. The retardance of diatoms is due to edge birefringence induced by the mismatch between the mounting medium and the silica of the shell. When using a high NA objective, the retardance measured around pores and markings is between 2 and 10 nm. The retardance pattern sensitively depends on the focus position and therefore is not suitable for calibrating the retardance and azimuth values of PolScope images. Test slides that include 8 different species with spacings ranging from 0.27 μm to 1.25 μm are available from Carolina Biological Supply Company (http://www.carolina.com/).
4. Test slides with lithographically made point and line objects, gratings of different periodicities, and other structures are an excellent way of testing the resolution and contrast transfer of microscope optics (Oldenbourg et al., 1996). Unfortunately, the

availability of these test slides is limited. Magnification standards that include repeating parallel lines with pitches of 0.5 μm and longer are commercially available from Geller MicroÅnalytical Laboratory, Topsfield, MA, (http://www.gellermicro.com/).

Sensitivity and noise sources

The sensitivity is determined by the smallest retardance that can reliably be measured with the PolScope. The sensitivity primarily depends on the noise level of PolScope images. We like to distinguish between two categories of noise sources: optical noise and measurement noise. In a static sample the two categories are easily distinguished by their spectral composition. Measurement noise typically is "white noise" changing randomly in PolScope images, both from pixel to pixel and from frame to frame. Optical noise, on the other hand, usually varies slowly from pixel to pixel and from frame to frame.

Optical noise originates from optical parts of the microscope that introduce unintended phase shifts in the polarized light beam leading to spurious sample retardance in PolScope images. Sources of optical noise include miscalibrated LCs of the universal compensator, differential transmission and phase shifts in microscope lenses, and optically anisotropic parts in the specimen itself. Miscalibrated LCs and polarization distortions introduced by optical components other than the specimen are effectively compensated using the background correction procedure described earlier. Unfortunately, the specimen itself is often a source of spurious birefringence. PolScope images of thick specimens typically show the retardance of the in-focus layer and of the out-of-focus parts together. The out-of-focus birefringence contributes to the optical noise and can reduce the sensitivity and accuracy of measuring the in-focus retardance in PolScope images. Suitable specimen preparations, avoiding the unnecessary stacking of specimen parts, for example, can reduce optical noise from out-of-focus parts. Also, out-of-focus retardance can sometimes be estimated and its effect on in-focus retardance can partially be removed (LaFountain and Oldenbourg, in press).

Measurement noise originates almost exclusively from shot noise of the light detected by the camera. Shot noise, also called photon statistics noise, derives from the inherent uncertainty in counting a finite number of photons (Taylor, 1997). All other electronic noise of modern CCD cameras, such as read noise, dark current and amplifier noise of the detector circuitry, are negligible compared to shot noise, because raw PolScope images are typically exposed to near full capacity of the CCD sensor chip. Current CCD sensors in cameras suitable for the PolScope have a typical single well capacity of around 18,000 electrons which correspond to 18,000 detected photons per image pixel. The uncertainty associated with detecting 18,000 photons is $\sqrt{18{,}000}$ and the signal to noise ratio is $S/N = 18{,}000/\sqrt{18{,}000} = 134$. This is the maximum S/N possible for this type of sensor chip. Detecting fewer than 18,000 photons decreases the S/N. For acquiring raw PolScope images, the camera pixels are filled to around 10,000 electrons, on average, leading to $S/N = 10{,}000/\sqrt{10{,}000} = 100$. Hence, the shot noise of raw PolScope images recorded with this type of camera leads to a relative intensity error of around 1%.

To make use of the full well capacity, the camera gain should be set to a minimum. With the gain set to a minimum, the analog to digital conversion in the camera converts the charge in a full well to a number near the upper limit of the digital range (either 8 or 12 bit). The camera off-

set should be adjusted with the light blocked from the camera. Adjust the offset so that the pixel reading is near but slightly larger than zero when no light is falling on the camera face plate.

The noise in measured intensity values leads to uncertainties in the calculated retardance and azimuth values. A more detailed analysis shows that the uncertainty of the measured specimen retardance is the Swing retardance multiplied by the relative intensity error. For example, an intensity shot noise of 1% and a Swing retardance of 16 nm leads to a retardance sensitivity of 0.16 nm.

It might be tempting to reduce the Swing retardance for improving the retardance sensitivity of the instrument. This is indeed possible but has some other pitfalls which are discussed later in connection with the effect of the extinction of the polarization optical train on retardance sensitivity.

The uncertainty in the measured azimuth angle increases inversely with the measured retardance value. For retardance values near zero, below the instrument's sensitivity, the shot noise in raw PolScope images results in a random azimuth angle that is uniformly distributed between 0 and 180°. The random distribution of azimuth values measured in specimen areas with zero retardance is indeed a good indicator that the background correction was successful. Azimuth values that are associated with retardance values that are larger than twice the sensitivity, typically have an uncertainty of about 1° to 2°.

The retardance sensitivity of a PolScope set-up can be estimated using the results of a calibration procedure. **Figure 2** shows the retardance and azimuth images of a clear specimen area after calibrating the PolScope in our laboratory equipped with high NA lenses and a digital CCD camera. Most retardance features are due to optical noise, as discussed under ***Background birefringence and how to correct it***. The optical noise is removed by the background correction procedure, as illustrated in **Figure 3**. In panel B of **Figure 3**, the background area around the cheek cell is black and shows no retardance, except for the measurement noise. The measurement noise is made visible by contrast enhancement of a small square region in the top left corner of panel B. The mean retardance background due to measurement noise in panel B is 0.08 nm, using 4 frame averaging.

The shot noise of a single raw PolScope image can be improved by averaging several camera frames that are captured in short succession while leaving the LC setting unchanged. Averaging N frames reduces the shot noise by a factor $1/\sqrt{N}$. The effectiveness of averaging, though, depends on the bit depth of a digital image. Gray scale images are typically pixel arrays, where each pixel is represented by either an 8 or 16 bit number. (8 bit integer values range between 0 and 255, 16 bit integers range between 0 and 65536). As discussed earlier, a well exposed, single frame has about 1% shot noise. Averaging 8 such frames reduces the shot noise to a level below the digital resolution of 8 bit. Therefore, averaging of more than 8 frames will improve image noise only if image data are stored using 16 bit per pixel.

Unfortunately, averaging requires time and therefore reduces the number of measurements that can be made within a certain time period. An alternative is to use a camera with a bigger well capacity, so that more photons can be captured before the camera frame is read-out.

The sensitivity also depends on the algorithm used to calculate the retardance and azimuth images. Recently, Michael Shribak in our laboratory has developed a series of algorithms that

use from two Settings to five Settings of the universal compensator (Shribak and Oldenbourg, 2003). Increasing the number of settings used increases the sensitivity of the measurements.

We have not yet mentioned the extinction of the polarization optical train in the PolScope. It is ultimately the extinction factor which determines the lower limit of the smallest retardance that can reliably be measured with the PolScope. As discussed earlier, the extinction factor is the ratio between the intensity with parallel polars (i.e. the total intensity of polarized light) and the light level passing the system when the polarizers are crossed (extinction = $I_{\parallel} / I_{\perp}$). The shot noise of the background light that passes even at extinction ultimately limits the sensitivity of the instrument. Here is a realistic numerical example: The ratio of the intensity with parallel polars to the intensity of one of the elliptical polarization settings (Settings 2 through 5) is $1/\sin^2(\chi/2)$, where χ is the swing retardance in degree. Assuming $\chi = 10.8$ (16 nm retardance), this ratio becomes 113. With high numerical aperture optics, on the other hand, we can achieve an extinction factor of around 500. Hence, the average intensity at the elliptical polarization settings is only 5 times higher than the average intensity at extinction. Reducing the swing value by a factor of 2 decreases the intensity at the elliptical settings by a factor of 4 and the background light becomes dominant for all PolScope Settings.

To measure the extinction of the PolScope include all optical components in the polarization optical train and view a clear area in the specimen. Then optimize the extinction setting, either by manually changing the LC settings in the software or by calibrating the instrument. Now reduce the lamp intensity and manually add half a wavelength retardance to the extinction setting (for example change Setting 1 from (λ/4, λ/2) to (3 λ/4, λ/2)). The light level on the camera will be very bright because the polarization optical train is now set for full transmission. If necessary reduce the lamp intensity further and measure the light level near the center of the image by choosing a short exposure time that results in medium gray pixels. Next, adjust the LCs back to the extinction setting and increase the exposure time until the light level registered by the camera is equal to the light level at full transmission. The ratio of the two exposure times gives the extinction factor.

Accuracy

Accuracy is related to systematic errors caused by incorrect system parameters. The system parameters that influence the accuracy of the measured specimen retardance include: the calibration of the Swing retardance, the proper mutual orientation of the birefringence axes of the retarder and polarizer components, and the linearity of the camera response. Another trivial but sometimes overlooked source of error is the azimuth reference angle entered into the PolScope software.

The optical components of the PolScope, including the camera, were manufactured and selected to satisfy a high standard of quality. Therefore, the accuracy of the instrument is expected to be of the same magnitude as the random errors introduced by the sources discussed earlier. If the accuracy of the complete set-up needs to be determined, though, we recommend to test and calibrate the instrument by measuring a test sample with known retardance and/or azimuth values. There are a number of points to consider when selecting the test sample and test procedure:

> As a test sample one can use a variety of birefringent objects with known retardance. Wave plates are available from microscope manufacturers and optical companies.

Use wave plates with low retardance such as quarter wave plates, or the λ/10 or λ/30 wave plate of a traditional Brace-Köhler compensator.

The retardance of a quartz wedge increases linearly with distance in the direction of the taper. The continuous, linear increase with distance provides a sensitive test for the linearity of the retardance measurement. The retardance of quartz wedges usually varies from near zero at one end of the wedge to several thousand nanometers at the other end. Beware, that the PolScope measures retardance values above half a wavelength ambiguously, as discussed under ***Retardance measurement***.

Use a set-up that is as complete as possible, including the imaging optics. That said, for some large test specimens like a commercial wave plate or quartz wedge it might be necessary to remove the objective and condenser lens and use the Bertrand lens to focus on the test specimen on the sample stage. The imaging optics should only have a minor influence on the accuracy of the instrument.

As azimuth standard one can use needle shaped crystals such as ammonium nitrate described in (Hartshorne and Stuart, 1960). While the retardance of the crystal depends on its size, its principal axes are exactly perpendicular and parallel to the crystal long axis.

When measuring a specimen, rotate it to several orientations and measure its retardance after each rotation. This will sensitively test the accuracy of the measured retardance and azimuth values versus known rotation angles (a makeshift rotation stage can be assembled from a Petri dish that is rotated in its stage holder).

Speed

The speed of the instrument is determined by the time it takes to acquire the raw PolScope images. During live retardance imaging, the time period also includes the calculation of the computed retardance and/or azimuth images. The calculation typically takes a small fraction of a second and cannot be influenced by the user. The time needed for acquiring the raw PolScope images, however, can vary substantially depending on a number of parameters including the specifications of instrument parts (such as LC settling time, lamp intensity, camera sensitivity) and the required resolution and sensitivity in the computed PolScope images. We have already discussed these parameters through out the text and usually pointed out their influence on the speed of acquisition. Here we summarize those points:

The LC settling time can account for more than 50% of the acquisition time. Currently, the universal compensator offered by CRi can be built with LCs that have settling times of either 150 ms or 30 ms.

When using a small swing retardance and seeking low shot noise to achieve high sensitivity, the exposure time, including frame averaging, can dominate the total acquisition time. Use a bright light source such as an arc lamp and a camera with high quantum efficiency to keep exposure times short.

Adjust the resolution of PolScope images to what is required for your experiment. Adjustments can be made by selecting the right objective lens, using a zoom lens before the camera and by either binning or selecting a sub-region of the CCD sensor. Decreasing the zoom factor, for example, is an effective way of increasing image

brightness and reducing exposure time. Binning or sub-region read-out can substantially reduce the camera read-out time and subsequent processing time.

Consider the sensitivity of PolScope images and what is required for your experiment. The sensitivity depends on the light level captured and the number of frames used for the calculation of retardance and azimuth images. Trading sensitivity can substantially increase the speed of measurement.

And use the Bertrand lens

Finally, I want to highly recommend the use of the Bertrand lens or telescope ocular for inspecting the optical path outside the immediate vicinity of the specimen. Many problems, such as misaligned optical components that cause shading, presence of dust particles that reduce the extinction, and air bubbles in immersion oil that can wreck havoc on the image are quickly recognized by looking down the optical path through a telescope ocular or with a Bertrand lens in place. The telescope ocular is exchanged against a regular eyepiece, while the Bertrand lens swings in the optical path somewhere between the objective and the ocular, which remains in place. In fact, if neither telescope ocular nor Bertrand lens are available, removing the regular ocular from the microscope and gazing down the empty tube (keep your eye about a hand width away from the tube end) lets you see the various optical components, albeit at low magnification. Usually we prefer the Bertrand lens which has a separate focusing mechanism and provides a magnified view of different optical planes. In many microscope designs, the Bertrand lens can also be used with the camera providing images, for example, of the objective back focal plane at different compensator settings (**Figure 5**).

When properly aligned for Köhler illumination, the objective back focal plane and the condenser front focal plane are simultaneously in focus (**for details see chapter on standard microscope alignments**). Hence, using the Bertrand lens the condenser aperture diaphragm can be adjusted to optimize the performance of the polarization optical train. For objectives with NAs of 0.7 or less, the condenser aperture should be set to limit the condenser NA to just under the objective NA. This setting reduces the chance of illuminating rays hitting the mounting of objective lens elements and thus contributing to stray light, which decreases image contrast and reduces extinction. For higher NA objectives, we typically set the condenser NA somewhat smaller than the objective NA to cut out high NA illumination rays which carry the highest polarization distortions. Keeping the condenser NA at not more than 1.0 improves considerably the extinction of the set-up when using immersion lenses.

Example Images and Movies

At the end we show images of living cells or cell components which illustrate the relationship between the measured retardance and specific cell structures. An introductory text to this relationship is available in Appendix III of the first edition of (Inoué, 1986). In addition to the references cited in the current chapter, we also refer to the many references on polarized light imaging listed in the same Appendix III of (Inoué, 1986). Also, in (Oldenbourg, 1999) we have discussed extensively the origin of birefringence in mitotic spindles.

The art and science of relating measured retardance and azimuth values to structural information on the molecular level of the specimen is only in its infancy. The potential information in PolScope images and time lapse movies is enormous. They can reveal the assembly and disas-

sembly of biological structures imaged in living cells that are functioning under physiological conditions. In some cases, such as the mitotic spindle, this promise has been partially realized and much has been learned about the reality of spindle fibers and the reversible assembly and disassembly of spindle filaments long before those notions were confirmed by other techniques (Inoué and Salmon, 1995). We are continuing the development of advanced instrumentation and of analytical methods for recording the intrinsic optical properties of biological materials and for interpreting them in terms of their molecular organization. **Figures 6 through 10** and **Movies 1 and 2** present examples of PolScope images and time lapse records of living cells and cell components illustrating the analytical strength and superb imaging that are made available by this technique.

Glossary of polarization optical terms

We give a brief introduction to polarization optical terms that are relevant for observations with the LC-PolScope. For a more detailed explanation of these and other terms which describe physical phenomena or optical devices we refer to excellent text books, monographs, and handbook articles such as (Hecht, 1998; Born and Wolf, 1980; Shurcliff, 1962; Chipman, 1995). See also Appendix III of the first edition of (Inoué, 1986).

Analyzer

An analyzer is a polarizer that is used to analyze the polarization state of light (see **Polarizer**)

Azimuth

The azimuth is an angle that refers to the orientation of the slow axis of a uniformly birefringent region. The azimuth image refers to the array of azimuth values of a birefringent specimen imaged with the LC-PolScope. The azimuth is typically measured from the horizontal orientation with values increasing for counterclockwise rotation. Angles range between 0 and 180° both of which indicate horizontal orientation.

Birefringence

Birefringence is a material property that can occur when there is molecular order, that is, when the average molecular orientation is non-random, as in crystals or in aligned polymeric materials such as those comprising the mitotic spindle. Molecular order usually renders the material optically anisotropic, leading to a refractive index that, in general, changes with the polarization of the light. For example, let us assume a beam of light passes through a mitotic spindle in a direction perpendicular to the spindle axis. The light that is polarized parallel to the spindle axis experiences a higher refractive index than the light that is polarized perpendicular to the spindle axis, i.e. the mitotic spindle is birefringent (due to the parallel alignment of microtubules (Sato et al., 1975)). For all birefringent materials, the difference between the two indices of refraction is called birefringence:

$$\textbf{birefringence} = \Delta n = n_{\parallel} - n_{\perp},$$

where $n_{\parallel}$ and $n_{\perp}$ are the refractive indices for light polarized parallel and perpendicular to one of the principal axes.

The LC-PolScope measures the relative phase shift between two orthogonally polarized light beams after they have traversed the birefringent material (see **Retardance**).

Compensator

A compensator is an optical device that includes one or more retarder plates and is commonly used to analyze the birefringence of a specimen. For a traditional polarizing microscope several types of compensators exist which typically use a single fixed retarder plate mounted in a mechanical rotation stage. With the help of a compensator one can distinguish between the slow and fast axis direction and measure the retardance of a birefringent object after orienting it with respect to the polarization axes of the microscope.

The LC-PolScope employs a universal compensator that includes two electro-optically controlled, variable retarder plates. Using the universal compensator one can measure the retardance and slow axis orientation of birefringent objects that have any orientation in the plane of focus.

Dichroism

Dichroism is a material property that can occur in absorbing materials with a non-random orientation of the light absorbing molecules. Dichroism refers to the difference in the absorption coefficients for light polarized parallel and perpendicular to the principal axis of alignment.

The measurement of optical anisotropy by the LC-PolScope is affected by the dichroism of absorbing materials. In non-absorbing, clear specimens, however, dichroism vanishes and birefringence is the dominant optical anisotropy measured by the LC-PolScope. Like absorption, dichroism is strongly wavelength dependent, while birefringence only weakly depends on wavelength.

Extinction

The extinction is defined as the ratio of maximum to minimum transmission of a beam of light that passes through a polarization optical train. Given a pair of linear polarizers, for example, the extinction is the ratio of intensities measured for parallel versus perpendicular orientation of the transmission axes of the polarizers (extinction = $I_{\parallel} / I_{\perp}$). In addition to the polarizers, the polarization optical train can also include other optical components which usually affect the extinction of the complete train. In a polarizing microscope the objective and condenser lens are located between the polarizers and significantly reduce the extinction of the whole set-up (see section on **Polarization optical components)**.

Fast axis

The fast axis describes an orientation in a birefringent material. For a given propagation direction, light polarized parallel to the fast axis travels the fastest in the material, and hence experiences the lowest refractive index. (See also **slow axis**)

Optic axis

The optic axis refers to a direction in a birefringent material. Light propagating along the optic axis does not change its polarization, hence for light propagating along the optic axis the birefringent material behaves as if it were optically isotropic.

Polarized light

A beam of light is said to be polarized when its electric field is distributed non-randomly in the plane perpendicular to the beam axis. In unpolarized light the orientation of the electric field is random and unpredictable. In partially polarized light, some fraction of the light is polarized, while the remaining fraction is unpolarized. Most natural light is unpolarized (sun, incandescent light), but can become partially or fully polarized by scattering, reflection, or interaction with

optically anisotropic materials. These phenomena are used to build devices to produce polarized light (see **Polarizer**).

Linearly polarized light

In a linearly polarized light beam the electric field is oriented along a single axis in the plane perpendicular to the propagation direction.

Circularly polarized light

In circularly polarized light the electric field direction rotates either clockwise (right-circularly) or counter-clockwise (left-circularly) when looking towards the source. While the field direction rotates, the field strength remains constant. Hence, the endpoint of the field vector describes a circle.

Elliptically polarized light

In elliptically polarized light, as in circularly polarized light, the electric field direction rotates either clockwise or counter-clockwise when looking towards the source. However, while the field direction rotates, the field strength varies in such a way that the end point of the field vector describes an ellipse. The ellipse has a long and short principal axis that are orthogonal to each other and have fixed orientation.

Any type of polarization (linear, circular or elliptical) can be transformed into any other type of polarization by means of polarizers and retarders.

Polarizer

A polarizer, sometimes called a polar, is a device that produces polarized light of a certain kind. The most common polar is a linear polarizer made from dichroic material (e.g. a plastic film with embedded, small iodine crystals that were aligned by stretching the plastic) that transmits light of one electric field direction while absorbing the orthogonal field direction. Crystal polarizers are made of birefringent crystals that split the light beam into orthogonal linear polarization components. A polarizer that produces circularly polarized light, a circular polarizer, is typically built from a linear polarizer followed by a quarter wave plate.

The LC-PolScope employs a universal compensator that can also be called a universal polarizer because it converts linear polarization into any other type of polarization by means of two variable retarders (see section **Polarization optical components**).

Retardance

Retardance is a measure of the relative optical path difference or phase change suffered by two orthogonal polarization components of light that has interacted with an optically anisotropic material. Retardance is the primary quantity measured by the LC-PolScope. Let's assume a nearly collimated beam of light traversing a birefringent material. The light component polarized parallel to the high refractive index axis travels at a slower speed through the birefringent material than the component polarized perpendicular to that axis. As a result, the two components, which were in phase when they entered the material, exit the material out of phase. The relative phase difference, expressed as the distance between the respective wave fronts, is called the retardance:

$$\textbf{retardance} = R = \left(n_{\parallel} - n_{\perp}\right) \cdot t = \Delta n \cdot t,$$

where t is the physical path length or thickness of the birefringent material. Hence, retardance has the dimension of a distance and is often expressed in nm. Sometimes it is convenient to express that distance as a fraction of the wavelength λ, such as λ/4 or λ/2. Retardance can also be defined as a differential phase angle, in which case λ/4 corresponds to 90° and λ/2 to 180° phase difference.

As a practical example we consider a mitotic spindle that is observed in a microscope that is equipped with low numerical aperture lenses (NA ≤ 0.5). When the spindle axis is contained in the focal plane, the illuminating and imaging beams run nearly perpendicular to the spindle axis. Under those conditions, the retardance measured in the center of the spindle is proportional to the average birefringence induced by the dense array of aligned spindle microtubules. To determine Δn one can estimate the thickness t by either focusing on spindle fibers located on top and bottom of the spindle and noting the distance between the two focus positions, or by measuring the lateral extend of the spindle when focusing through its center. The latter approach assumes a rotationally symmetric shape of the spindle. Typical values for the spindle retardance of crane fly spermatocytes (**Figure 7**) and of other cells is 3 to 5 nm and the spindle diameter is about 30 to 40 μm, leading to an average birefringence of around 10^{-4}. Workers (Sato et al., 1975) found that the retardance value of the spindle was largely independent of the NA for imaging systems using NA ≤ 0.5.

On the other hand, when using an imaging set-up that employs high NA optics (NA > 0.5) for illuminating and imaging the sample, the measured retardance takes on a somewhat different context. For example, the retardance measured in the center of a microtubule image recorded with the LC-PolScope equipped with a high numerical aperture objective and condenser lens is 0.07 nm (**Figure 6**). A detailed study showed that the peak retardance decreased inversely with the NA of the lenses. However, the retardance integrated over the cross section of the microtubule image was independent of the NA (Oldenbourg et al., 1998). While a conceptual understanding of the measured retardance of submicroscopic filaments has been worked out in the aforementioned publication, a detailed theory of these and other findings about the retardance measured with high NA optics is still missing.

Retarder

A retarder or waveplate is an optical device that is typically made of a birefringent plate. The retardance of the plate is the product of the birefringence of the material and the thickness of the plate. Fixed retarder plates are either cut from crystalline materials such as quartz, calcite, mica, or they are made of aligned polymeric material. If the retardance of the plate is λ/4, for example, the retarder is called a quarter waveplate.

A variable retarder can be made from a liquid crystal device. A thin layer of highly birefringent liquid crystal material is sandwiched between two glass windows that each bear a transparent electrode. A voltage applied between the electrodes produces an electric field across the liquid crystal layer that reorients the liquid crystal molecules. This reorientation changes the birefringence of the layer without affecting its slow axis direction or thickness.

Slow axis

The slow axis describes an orientation in a birefringent material. For a given propagation direction, light polarized parallel to the slow axis travels the slowest in the material,and hence experiences the highest refractive index (see also **fast axis**).

Waveplate

See retarder

Acknowledgments

The wisdom collected in this chapter is the result of more than 14 years of designing and building microscope instrumentation and working with microscopes to study living cells. In all these years I had the privilege and pleasure to interact and work with a superb group of people, dedicated to building the best instruments and using them in innovative ways to solve interesting problems in biology and medicine. Their contributions justify the "we" in the text above; the mistakes, though, are mine alone. I would like to thank them all for their support. The names are too numerous to list them all, but I would like to mention the colleagues and friends from whom I learned the most, by both encouragement and challenge and by contributing to the fun of working together: Shinya Inoué, who set me on the path, Bob Knudson, who magically creates the parts, Ted Salmon and Phong Tran, who were early believers, Kaoru Katoh, David Keefe, and Lin Liu, who reaped the first fruits, Michael Shribak, who is unleashing a flurry of innovations, Grant Harris, who is bridging the digital divide, Jim LaFountain, who opened my eyes to the beauty of crane flies, Cliff Hoyt and Cathy Boutin, who bring this technology to the masses, and Nannette, Marie and Helena, who give meaning and a place to call home. I also would like to thank Michael Shribak, Jim Valles and Shinya Inoué for comments on parts of the manuscript. Finally, we couldn't do without the financial support from the National Institute of General Medical Sciences and from the National Institute of Biomedical Imaging and Bioengineering through grants GM49210 and EB002045, respectively.

References

Ambronn, H. and Frey, A. (1926). Das Polarisationsmikroskop, seine Anwendung in der Kolloidforschung und in der Färberei. Leipzig: Akademischer Verlag.

Born, M. and Wolf, E. (1980). Principles of Optics. Elmsford, N.Y.: Pergamon Press.

Chipman, R. A. (1995). Polarimetry. In *Handbook of Optics*, vol. 2 (ed. M. Bass), pp. 22.1-22.37. New York: McGraw-Hill, Inc.

Frey-Wyssling, A. (1953). Submicroscopic Morphology of Protoplasm. Amsterdam: Elsevier.

Hartshorne, N. H. and Stuart, A. (1960). Crystals and the Polarising Microscope: A Handbook for Chemists and Others. London: Arnold.

Hecht, E. (1998). Optics. Reading MA: Addison-Wesley.

Inoué, S. (1952). Studies on depolarization of light at microscope lens surfaces. I. The origin of stray light by rotation at the lens surfaces. *Experimental Cell Research* **3**, 199-208.

Inoué, S. (1953). Polarization optical studies of the mitotic spindle. I. The demonstration of spindle fibers in living cells. *Chromosoma* **5**, 487-500.

Inoué, S. (1986). Video Microscopy. New York: Plenum Press.

Inoué, S. (2002). Polarization Microscopy. In *Current Protocols in Cell Biology*, vol. 1 (Suppl. 13) (ed. J. S. Bonifacino M. Dasso J. B. Harford J. Lippincott-Schwartz and K. M. Yamada), pp. 4.9.1-4.9.27. New York: John Wiley & Sons.

Inoué, S. and Dan, K. (1951). Birefringence of the dividing cell. *Journal of Morphology* **89**, 423-456.

Inoué, S. and Hyde, W. L. (1957). Studies on depolarization of light at microscope lens surfaces II. The simultaneous realization of high resolution and high sensitivity with the polarizing microscope. *J. Biophys. Biochem. Cytol.* **3**, 831-838.

Inoué, S. and Oldenbourg, R. (1995). Microscopes. In *Handbook of Optics*, vol. 2 (ed. M. Bass), pp. 17.1-17.52. New York: McGraw-Hill, Inc.

Inoué, S. and Salmon, E. D. (1995). Force generation by microtubule assembly/disassembly in mitosis and related movements. *Molecular Biology of the Cell* **6**, 1619-1640.

Inoué, S. and Sato, H. (1966). Deoxyribonucleic acid arrangement in living sperm. In *Molecular Architecture in Cell Physiology*, (ed. T. Hayashi and A. G. Szent-Gyorgyi), pp. 209-248. Englewood Cliffs, NJ: Prentice Hall.

Inoué, S., Shimomura, O., Goda, M., Shribak, M. and Tran, P. T. (2002). Fluorescence polarization of green fluorescence protein. *Proc Natl Acad Sci U S A* **99**, 4272-4277.

Inoué, S. and Spring, K. R. (1997). Video Microscopy. New York: Plenum Press.

Katoh, K., Hammar, K., Smith, P. J. S. and Oldenbourg, R. (1999). Birefringence imaging directly reveals architectural dynamics of filamentous actin in living growth cones. *Molecular Biology of the Cell* **10**, 197-210.

LaFountain, J. R., Jr and Oldenbourg, R. (in press). Maloriented bivalents are positioned at the spindle equator with more kinetochore microtubules to one pole than to the other. *Molecular Biology of the Cell*.

Liu, L., Oldenbourg, R., Trimarchi, J. R. and Keefe, D. L. (2000). A reliable, noninvasive technique for spindle imaging and enucleation of mammalian oocytes. *Nature Biotechnology* **18**, 223-225.

Mitchison, J. M. (1950). Birefringence of Amœbæ. *Nature* **166**, 313-315.

Oldenbourg, R. (1999). Polarized light microscopy of spindles. In *Methods in Cell Biology; Mitosis and Meiosis*, vol. 61 (ed. C. L. Rieder), pp. 175-208. San Diego: Academic Press.

Oldenbourg, R., Inoué, S., Tiberio, R., Stemmer, A., Mei, G. and Skvarla, M. (1996). Standard test targets for high resolution light microscopy. In *Nanofabrication and Biosystems: Integrating Material Science, Engineering and Biology*, (ed. H. C. Hoch L. W. Jelinsky and H. Craighead), pp. 123-138. Cambridge, England: Cambridge University Press.

Oldenbourg, R. and Mei, G. (1996). Polarized Light Microscopy. In *US Patent, Number 5,521,705*, (ed. USA: Marine Biological Laboratory (Woods Hole, MA).

Oldenbourg, R., Salmon, E. D. and Tran, P. T. (1998). Birefringence of single and bundled microtubules. *Biophysical Journal* **74**, 645-654.

Oldenbourg, R. and Török, P. (2000). Point spread functions of a polarizing microscope equipped with high numerical aperture lenses. *Applied Optics* **39**, 6325-6331.

Palazzo, R. E., Vaisberg, E., Cole, R. W. and Rieder, C. L. (1992). Centriole duplication in lysates of *Spisula solidissima* oocytes. *Science* **256**, 219-221.

Peterman, E. J. G., Sosa, H., Goldstein, L. S. B. and Moerner, W. E. (2001). Polarized fluorescence microscopy of individual and many kinesin motors bound to axonemal microtubules. *Biophysical Journal* **81**, 2851-2863.

Rieder, C. L. and Khodjakov, A. (2003). Mitosis through the microscope: advances in seeing inside live dividing cells. *Science* **300**, 91-6.

Salmon, E. D. and Tran, P. T. (1998). High-resolution video-enhanced differential interference contrast (VE-DIC) light microscopy. *Methods in Cell Biology* **56**, 153-184.

Sase, I., Miyata, H., Ishiwata, S. I. and Kinosita, K., JR. (1997). Axial rotation of sliding actin filaments revealed by single-fluorophore imaging. *Proc Natl Acad Sci U S A* **94**, 5646-5650.

Sato, H., Ellis, G. W. and Inoué, S. (1975). Microtubular origin of mitotic spindle form birefringence Demonstration of the applicability of Wiener's equation. *Journal of Cell Biology* **67**, 501-517.

Schmidt, W. J. (1937). Die Doppelbrechung von Karyoplasma, Zytoplasma und Metaplasma. Berlin: Bornträger.

Shribak, M., Inoué, S. and Oldenbourg, R. (2002). Polarization aberrations caused by differential transmission and phase shift in high NA lenses: theory, measurement and rectification. *Optical Engineering* **41**, 943-954.

Shribak, M. and Oldenbourg, R. (2003). Techniques for fast and sensitive measurements of two-dimensional birefringence distributions. *Applied Optics* **42**, 3009-3017.

Shurcliff, W. A. (1962). Polarized Light, Production and Use. Cambridge, MA: Harvard University Press.

Sluder, G. and Wolf, D. E. (1998). Video Microscopy. In *Methods in Cell Biology*, vol. 56 (ed. L. Wilson and P. Matsudaira). San Diego: Academic Press.

Swann, M. M. and Mitchison, J. M. (1950). Refinements in polarized light microscopy. *Journal of Experimental Biology* **27**, 226-237.

Taylor, J. R. (1997). An Introduction to Error analysis. Sausalito, California: University Science Books.

Török, P. (2000). Imaging of small birefringent objects by polarised light conventional and confocal microscopes. *Optics Communications* **181**, 7-18.

Warshaw, D. M., Hayes, E., Gaffney, D., Lauzon, A.-M., Wu, J., Kennedy, G., Trybus, K., Lowey, S. and Berger, C. (1998). Myosin conformational states determined by single fluorophore polarization. *Proc Natl Acad Sci U S A* **95**, 8034-8039.

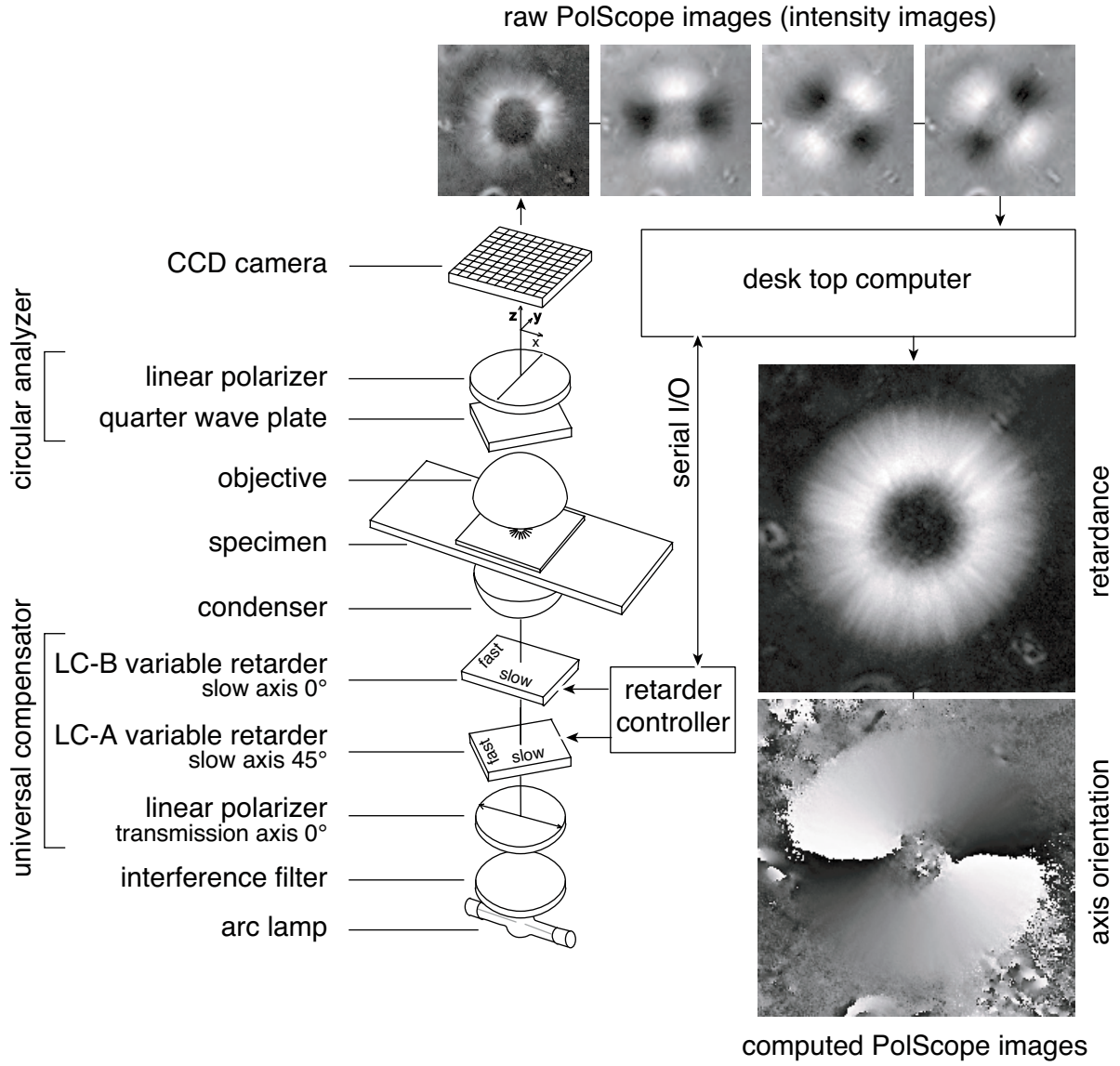

Figure 1. Schematic of the LC-PolScope. The optical design (left) builds on the traditional polarized light microscope with the conventional compensator replaced by two variable retarders LC-A and LC-B. The polarization analyzer passes circularly polarized light and is typically built from a linear polarizer and a quarter wave plate. Images of the specimen (top row, aster isolated from surf clam egg) are captured at four predetermined retarder settings which cause the specimen to be illuminated with circularly polarized light (1st, left most image) and with elliptically polarized light of different axis orientations (2nd to 4th image). Based on the raw PolScope images, the desk top computer calculates the retardance image and the axis orientation or azimuth image shown on the lower right.

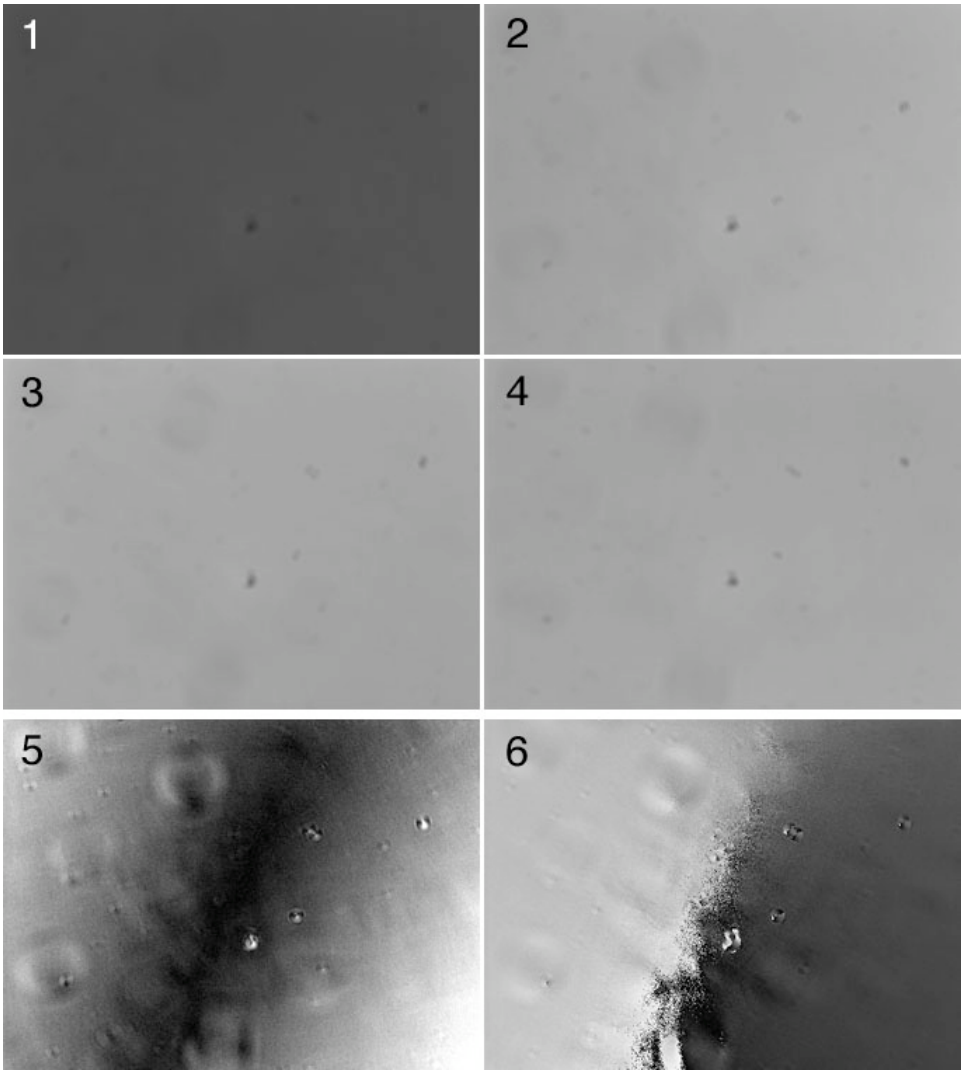

Figure 2. PolScope images acquired of an empty area of a thin aqueous layer sandwiched between a microscope slide and coverslip. The focus was set to the center of the aqueous layer which lacks any distinct feature. **Panels 1** to **4** show raw PolScope images representing the recorded intensities from the empty area using universal compensator Settings 1 through 4. **Panel 5** shows the computed retardance image, black representing zero retardance and white 1.5 nm retardance. **Panel 6** shows the azimuth image (black is 0° and white is 180°). These so-called background images illustrate the retardance and its azimuth contributed by components of the optical set-up other than the focused layer in the specimen (see text). (Oil immersion Plan Apochromat objective 60x/1.4 NA, and oil immersion condenser).

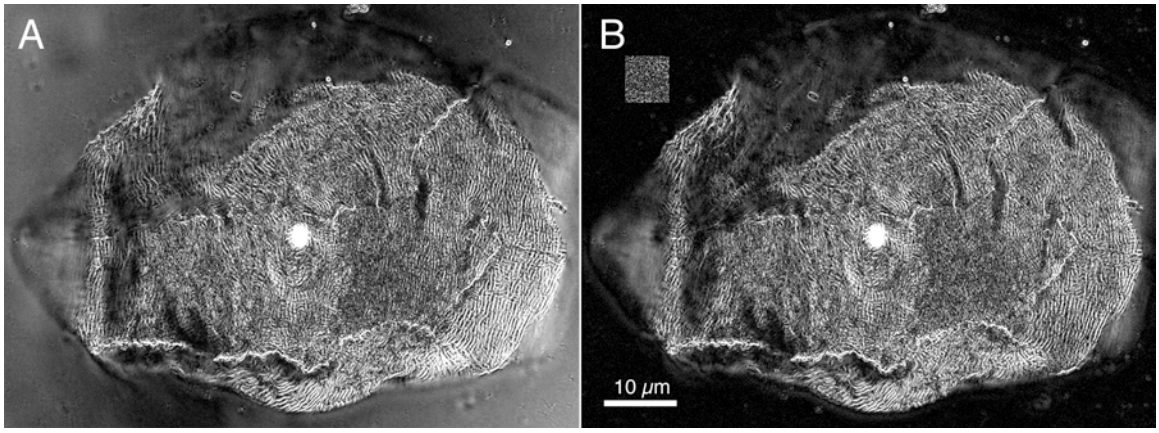

Figure 3. Retardance images of a buccal mucosal cell (cheek cell) illustrating the effect of background retardance and of its removal using background correction (same specimen preparation was used for Figure 2). Panel **A** shows the retardance image (white is 3 nm retardance) without background correction and panel **B** with background correction. In panel B the birefringence of cell structures such as the fine ridges on the cell surface are faithfully reproduced. The clear area around the cell is dark, showing no retardance, as expected. In the top left corner of panel B a square region of the background is contrast enhanced (white is 0.3 nm retardance) to illustrate the measurement noise as discussed in ***Sensitivity and noise sources***. In panel A the retardance of the cell is contaminated by the background retardance. The background retardance is shown separately in Fig 2.

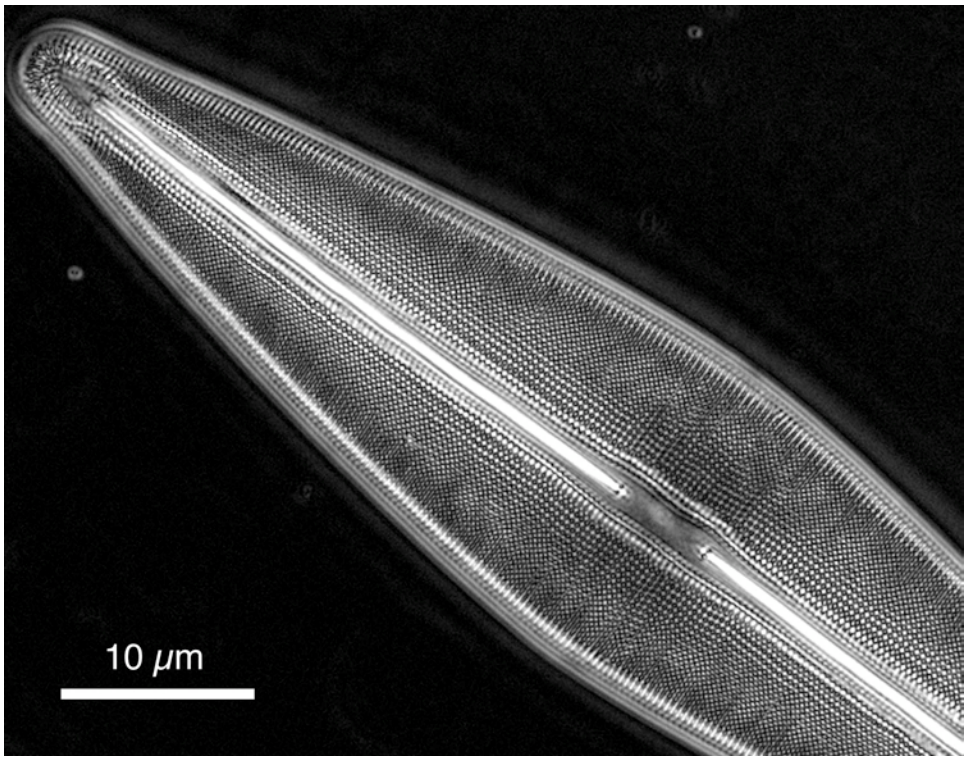

Figure 4. Retardance image of a *Frustulia rhomboides* diatom shell. Rows of pores are 0.29 μm apart. The diatom was imaged with a Plan Apochromat 60x/1.4 NA oil immersion objective and Plan Achromat oil immersion condenser, with the condenser aperture set to about 1.0 NA. White corresponds to 4 nm retardance.

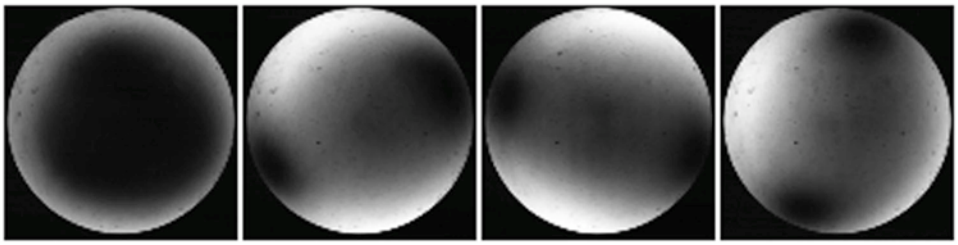

Figure 5. Objective lens back aperture of the PolScope equipped with high NA oil immersion objective and condenser lenses. Images, from left to right, were taken using Settings 1 through 4 of the universal compensator and with a Bertrand lens in the optical path. The images demonstrate the nature and appearance of polarization distortions introduced by high numerical aperture lenses. The full diameter of the aperture corresponds to 1.4 NA of a Plan Apo 60x/1.4 NA oil immersion objective and apochromat condenser of same NA, both selected for low polarization distortions; homogeneous immersion of n=1.52 between condenser and objective; no specimen in optical path. For a discussion of polarization aberrations in high NA optical systems and ways to rectify them, see (Shribak et al., 2002).

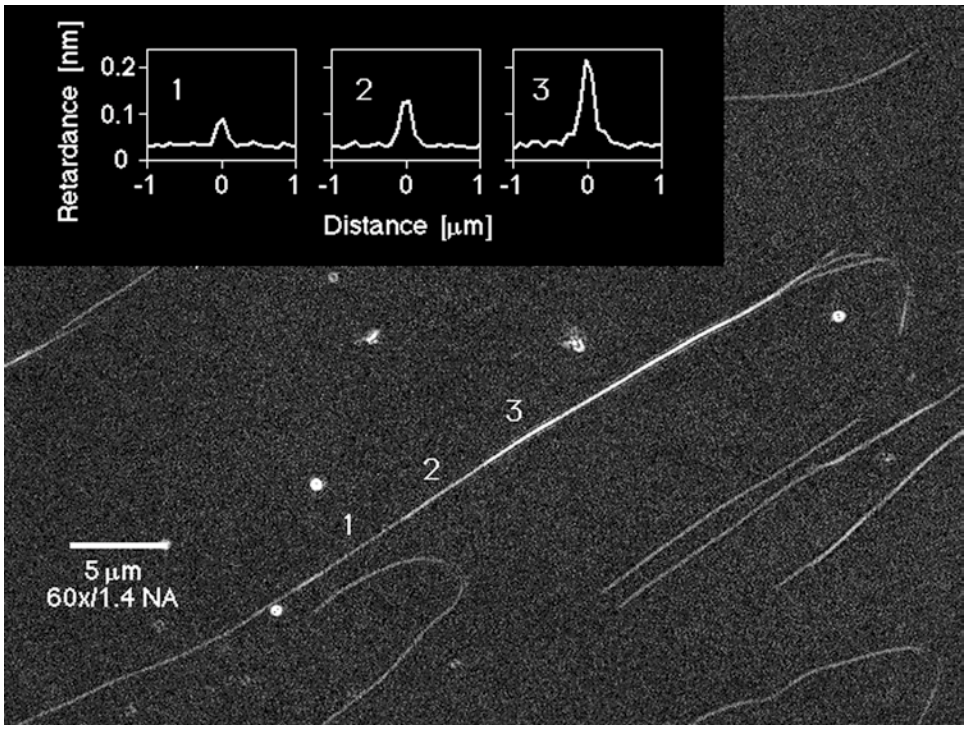

Figure 6. Spontaneously assembled microtubules, stabilized with taxol, adhere to the cover glass surface and were imaged with the LC- PolScope (retardance image). Most filaments are single microtubules (MT), with the exception of one bundle containing one, two and three MTs. The inset shows line scans across the filament axis at locations with one, two, and three MTs. Note on the top right end, the bundle sprays into three individual microtubules. (Reproduced with permission from (Oldenbourg et al., 1998)).

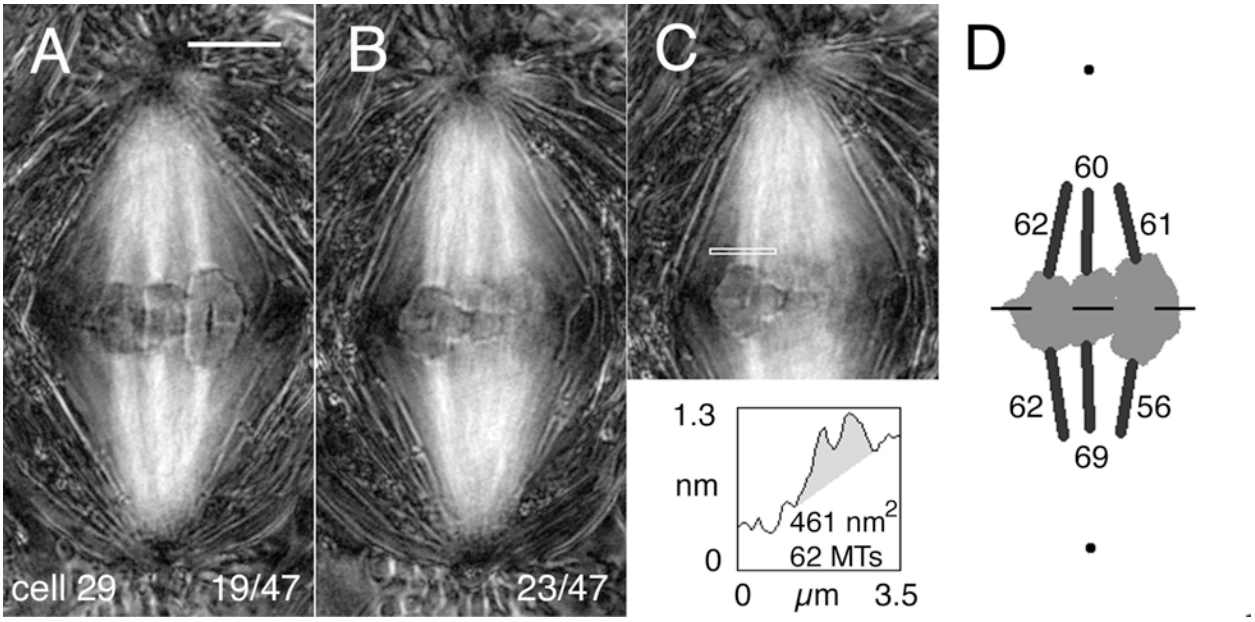

Figure 7. Birefringent kinetochore fibers in a spermatocyte of the crane fly *Nephrotoma suturalis* imaged with the LC-PolScope. **(A)** and **(B)** are two sections from a series of optical sections made through the cell at focus steps of 0.26μm. Lower right: slice number/total slices in the focus series. In viewing these polarized light images, brightness represents the retardance (black = 0nm and white = 2.5nm retardance), irrespective of the orientation of the principal axis. Bar, 5μm.

(C) A duplicate image of (B) including the line from which retardance area data were obtained. The shaded area in the plot is the retardance area (461nm^2) of the fiber, which was evaluated for the number of kinetochore microtubules (62).

(D) The metaphase positions of the three bivalent chromosomes in this cell upon projection of all images within the Z-focus series to make a 2-D profile. Two dots indicate the positions of the flagellar basal bodies within the centrosomes at the two spindle poles. The numbers on each kinetochore fiber indicate the number of kinetochore microtubules in that fiber, based on retardance area analysis (LaFountain and Oldenbourg, in press).

Movie 1 Meiosis I in spermatocyte of the crane fly Nephrotoma suturalis (first published as web supplement to the article (Rieder and Khodjakov, 2003)).

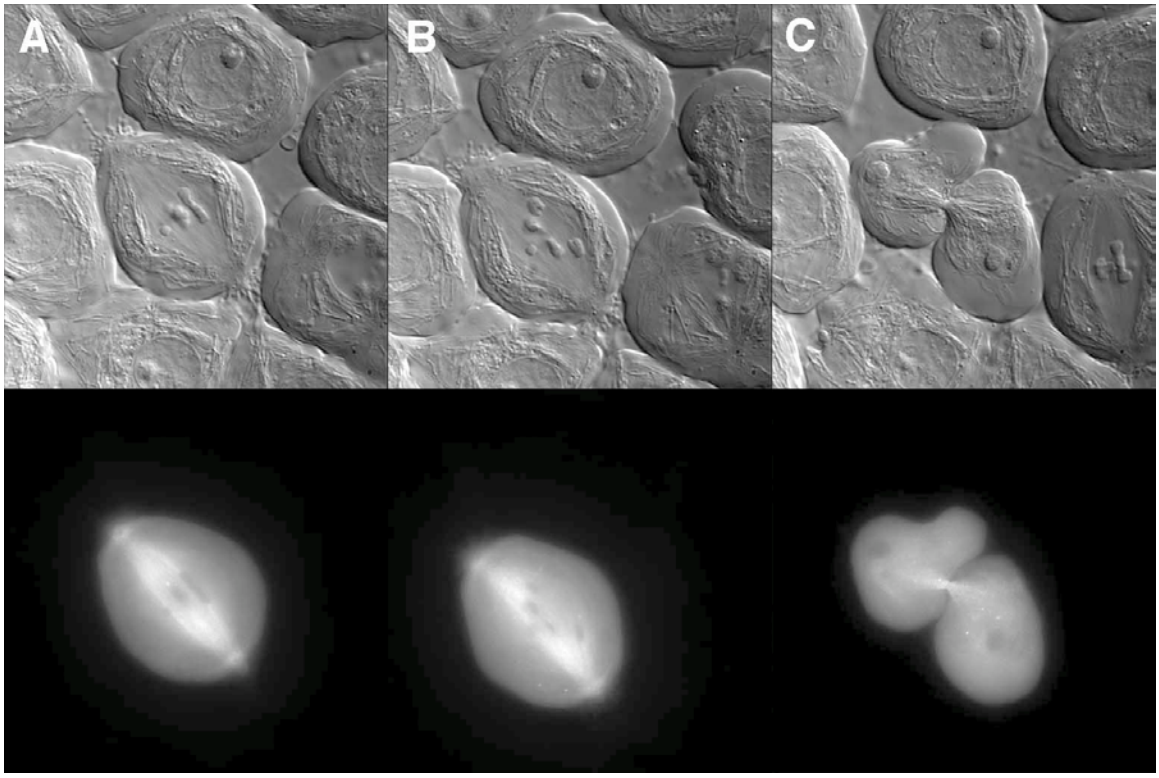

Figure 8. Crane-fly spermatocytes viewed with differential interference contrast and fluorescence microscopy, two imaging modes that are complementary to the PolScope (Figure 7). Spindle microtubules are fluorescently labeled following injection of rhodamine-tubulin into the cytoplasm of one spermatocyte. A field of cells recorded with DIC optics is presented in A, B, and C. In the paired fluorescence images, the kinetochore fibers of the injected cell appear prominent on a less fluorescent background, which contains unassembled rhodamine-tubulin subunits. Centrosomes are also quite fluorescent. Kinetochore microtubules shorten during anaphase A. as the injected cell progresses through anaphase and then through cytokinesis. The figure is courtesy of Dr. James R. LaFountain Jr. of the University at Buffalo.

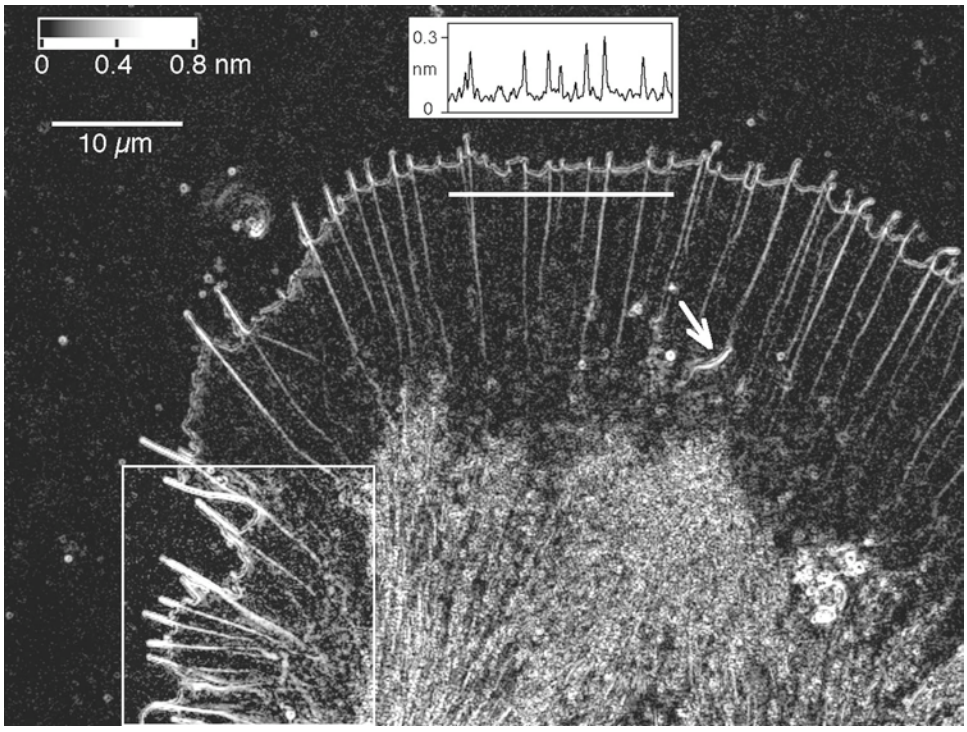

Figure 9. Birefringent fine structure in the living growth cone of *Aplysia* Bag Cell neuron. This retardance image, recorded with the LC-PolScope, shows the peripheral lamellar domain containing radially aligned birefringent fibers which end in filopodia at the leading edge of the growth cone. The graph in the top center shows the retardance, in nm, measured along a 3 pixel wide strip, indicated by a horizontal white bar. The measured peak retardance in radial actin fibers can be interpreted in terms of the number of actin filaments in a fiber. Near the bottom, the image shows the central domain, which is filled with vesicles and highly birefringent microtubule bundles. On the bottom left, a region is outlined and its contrast is enhanced to show clearly the diffuse birefringent patches of partially aligned actin networks located mainly in the transition region between the thin lamellar and thicker central domain. The arrow near the center of the image points to a spontaneously formed intrapodium with its strongly birefringent tail formed by parallel actin arrays. The image is one frame of a time-lapse record that reveals the architectural dynamics of the cytoskeleton including the formation of new filopodia and radial fibers and the continuous retrograde flow of birefringent elements in the peripheral domain. The top left corner of the image contains a gray wedge with retardance scale, the time in minutes and seconds elapsed since the first frame of the movie and a bar indicating the length scale. (Reproduced with permission from (Katoh et al., 1999))

Movie 2. Birefringent fine structure in the living growth cone of an Aplysia bag cell neuron.

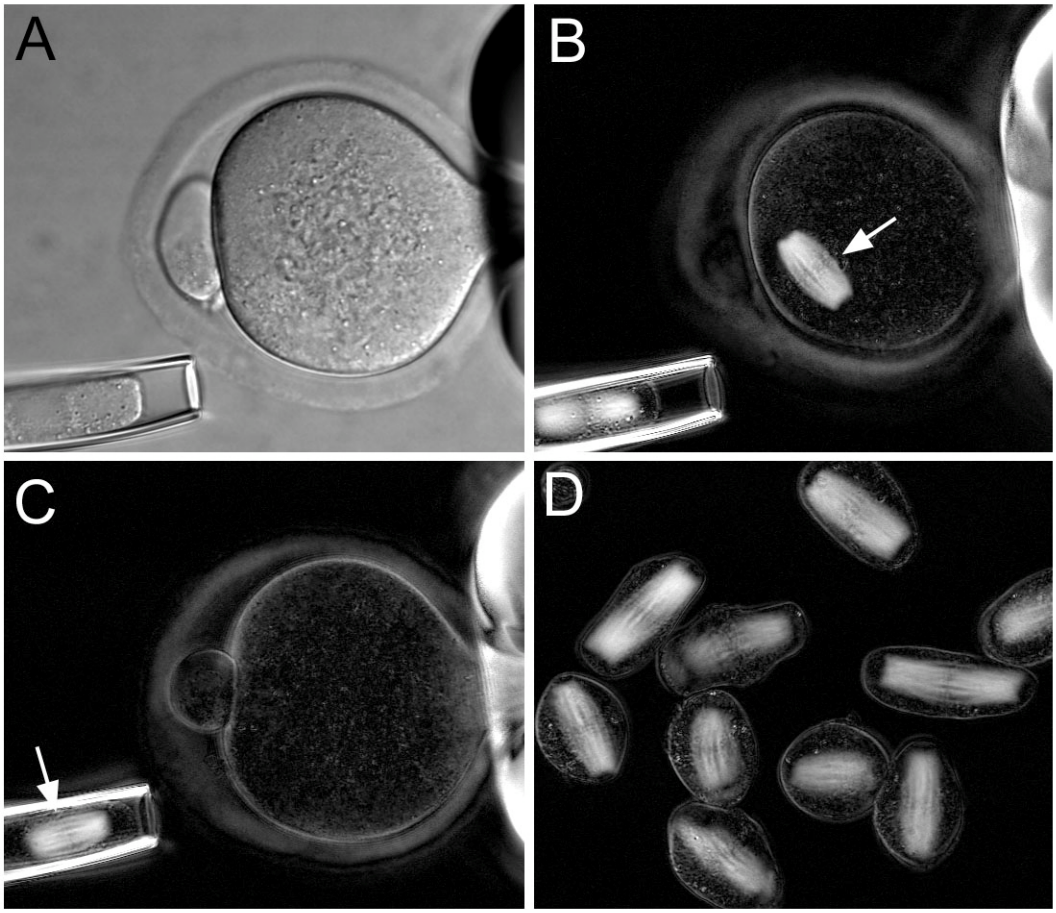

Figure 10. Mouse oocyte and enucleated spindles. **(A)** mouse oocyte held in place by gentle suction of a holding pipette (oocyte diameter approx. 75 μm, differential interference contrast microscopy); **(B)** Retardance image of the same oocyte, with birefringent spindle of meiosis II (white arrow); **(C)** The spindle (arrow) is aspirated into an enucleation pipette; **(D)** a batch of enucleated spindles and chromosomal karyoplasts. Chromosomes are aligned in the middle of spindles. The figure is courtesy of Lin Liu of the Marine Biological Laboratory (for more detailed information see (Liu et al., 2000)).